ANALYSIS AND INTERPRETATION OF PRESSURE TRANSIENT TEST DATA BY RECENT ROBUST DECONVOLUTION METHODS

by

Muhammad Izzatullah Mohd Mustafa

13238

A PROJECT DISSERTATION

SUBMITTED TO THE DEPARTMENT OF PETROLEUM ENGINEERING

IN PARTIAL FULFILLMENT OF THE REQUIREMENTS FOR THE BACHELOR DEGREE IN PETROLEUM ENGINEERING

Supervised by Prof. Dr. Mustafa Onur

Universiti Teknologi PETRONAS

Bandar Seri Iskandar

31750 Tronoh

Perak Darul Ridzuan

CERTIFICATION OF APPROVAL

ANALYSIS AND INTERPRETATION OF PRESSURE TRANSIENT TEST DATA BY RECENT ROBUST DECONVOLUTION METHODS

by

Muhammad Izzatullah Mohd Mustafa

13238

A PROJECT DISSERTATION

SUBMITTED TO THE DEPARTMENT OF PETROLEUM ENGINEERING

IN PARTIAL FULFILLMENT OF THE REQUIREMENTS FOR THE BACHELOR DEGREE IN PETROLEUM ENGINEERING

Approved by,

……..

(Prof. Dr. Mustafa Onur)

Universiti Teknologi PETRONAS

Bandar Seri Iskandar

31750 Tronoh

Perak Darul Ridzuan

Certification of Originality

This is to certify that I am responsible for the work submitted in this project, that the original work is my own except as specified in the references and acknowledgements, and that the original work contained herein have not been undertaken or done by unspecified sources or persons.

_____

MUHAMMAD IZZATULLAH MOHD MUSTAFA

Abstract

Recently, the robust deconvolution algorithms that tolerate high levels of errors in pressure and rate than the previous deconvolution algorithms have been introduced in the literature. The recently developed deconvolution method by von Schroeter *et al*. (2002, 2004) and its variants later developed by Levitan (2005) and Pimonov et al. (2010) appear to offer robustness to the long-standing deconvolution problem and make deconvolution a viable tool to pressure transient and production data analysis. Now, most commercial software incorporates either the method developed by von Schroeter et al. or its variants developed by Levitan (2005) and Pimonov et al. (2010). However, there are some algorithmic parameters that need to be carefully selected to produce meaningful constant-rate (or deconvolved) responses from these algorithms to avoid misinterpretation of the data leading to misidentification of the unknown system. In this work, by using the recent robust deconvolution algorithm of Pimonov et al. and/or the ones implemented in Weatherford PanSystem Well Test Software, the effects of the algorithmic parameters (including error levels in pressure and rate data, and the curvature constraint value) as well as the initial pressure on the deconvolved responses are investigated. Several synthetic and field test data are used to illustrate the effects of the algorithmic parameters on the deconvolved responses as well as the importance of the deconvolution in analysis and interpretation of pressure transient data.

Acknowledgments

First of all, I would like to express my appreciation to my advisor, Prof. Dr. Mustafa Onur. He provided me with great experience, guidance and continuous support during my Final Year Project (FYP). I owe many thanks to Universiti Teknologi PETRONAS for providing all the facilities in research especially the licensed Weatherford PanSystem version 3.5 which be using throughout the FYP in this deconvolution study.

I would like to thank my mentor at Schlumberger Ltd, Chin Loong Seah, who provided great help and advices throughout my final year especially in completing this FYP.

I would like to thank my family for their support during these years. I want to especially thank my mother, Norini Ahmad, and also my father, Mohd Mustafa, who has devoted tremendous support and encouragement for my education. Also, thanks to my special one, Irene Ling Fun Yen, who gave much support during my undergraduate studies by keep giving new ideas towards my success.

Finally, I would also like to thank all my friends in Petroleum Engineering Department; Moktar Abdellahi Bebaha, Muhammad Izhan Noorzi, Nur Syaffiqa Mohamad Ruzlan, Hussam Eldin Ali, Mohamed Yousry Ahmed Hussien, Nur Syazwani Moktar, Khairunnisa Saharuddin, Mosab Mohamed, and Juhairi Aris who gave much support during my undergraduate studies.

Contents

Certification of Approval **i**

Certification of Originality **ii**

Abstract **iii**

Acknowledgement **iv**

1 Introduction **1**

1.1 Background of Study 1

1.2 Problem Statement 2

1.3 Objectives 3

1.4 Scope of Study 3

2 Literature Review **4**

2.1 Deconvolution Concept and Basic 4

2.2 The Development of Deconvolution Algorithm 6

3 Methodology **8**

3.1 Research Methodology Flow Chart 8

3.2 Project Gantt Charts 10

3.3 Software 11

3.1.1 Pimonov et al. (2010) codes 11

3.1.2 Weatherford Pansystem 11

4 Results and Discussion **12**

4.1 Sensitivity study using Simulated Data 12

4.1.1 Synthetic Example 1 12

4.1.2 Synthetic Example 2 17

4.1.3 Synthetic Example 3 21

4.1.4 Synthetic Example 4 32

4.1.4.1 Case 1 36

4.1.4.2 Case 2 39

4.1.4.3 Case 3 42

5 Conclusions and Recommendations **47**

References **49**

List of Tables

4.1	Input Parameters for Synthetic Example 1 and Example 2	14
4.2	Input Parameters for Synthetic Example 3	23
4.3	Deconvolution parameters used for the synthetic example 3 (Pimonov et al. algorithm)	24
4.4	Deconvolution parameters used for the synthetic example 3 (von Schroeter et al. algorithm)	29
4.5	Input Parameters for Synthetic Example 4	33
4.6	Estimated initial pressure values generated by deconvolution algorithm for Case 1	39
4.7	Estimated initial pressure values generated by deconvolution algorithm for Case 2	42
4.8	Estimated initial pressure values generated by deconvolution algorithm for Case 3	45

List of Figures

2.1	A Schematic representation of the deconvolution operation (Kuchuk et al. 2010)	4
2.2	Pressure – rate convolution and deconvolution	6
2.3	Timeline of deconvolution development in petroleum engineering literature	7
3.1	Flow chart on research methodology	9
3.2	FYP 1 Gantt Chart	10
3.3	FYP 2 Gantt Chart	10
4.1	Reservoir/well configuration for synthetic example	13
4.2	Pressure data for Synthetic Example 1	13
4.3	Rate data for the Synthetic Example 1	14
4.4	The pressure responses obtained by deconvolution of the buildup period; Synthetic Example 1	16
4.5	Comparison between true and 40 nodes of Pimonov et al. models.	16
4.6	The pressure responses obtained by deconvolution of the buildup period without optimize flow rates; Synthetic Example 2	18
4.7	The pressure responses obtained by deconvolution of the buildup period with optimize flow rates; Synthetic Example 2	19
4.8	Comparison between true and 40 nodes of Weatherford PanSystem models.	20
4.9	Pressure data for Synthetic Example 3	21
4.10	Rate data for Synthetic Example 3	22
4.11	Reservoir geometry for Synthetic Example 3	22
4.12	True pressure history and corrupted pressure history (contains noise)	25
4.13	True flow rate history and corrupted flow rate history (contains noise)	25
4.14	True pressure unit response and its derivatives	26

4.15	Comparison of deconvolution responses and derivatives with true and five different cases of parameters given in Table 4.3 for synthetic example 3.	27
4.16	Comparison of deconvolution responses and derivatives with true and five different cases of parameters given in Table 4.4 for synthetic example 3.	30
4.17	Reservoir Geometry for Synthetic Example 4	32
4.18	Pressure data for Synthetic Example 4	34
4.19	Flow rate data for Synthetic Example 4	35
4.20	True deconvolved unit response and its derivative for Synthetic Example 4	36
4.21	Comparison of deconvolution responses for different known initial reservoir pressures (Case 1)	37
4.22	Comparison of deconvolution responses for different unknown initial reservoir pressures (Case 1)	38
4.23	Comparison of deconvolution responses for different known initial reservoir pressures (Case 2)	40
4.24	Comparison of deconvolution responses for different unknown initial reservoir pressures (Case 2)	41
4.25	Comparison of deconvolution responses for different known initial reservoir pressures (Case 3)	44
4.26	Comparison of deconvolution responses for different unknown initial reservoir pressures (Case 3)	45

Chapter 1

Introduction

1.1 Background of Study

Deconvolution provides the equivalent constant rate/pressure response of the well/reservoir system affected by variable flow rates/pressures and hence eases the system identification and data interpretation. By using Deconvolution analysis, one can extract more information about the well/reservoir system, regarding reservoir boundaries and oil and gas volumes supported by well test data. Such information is vital for making decisions for appraising the fields and reducing the overall costs of the reservoir appraisal and development programs. However, applying deconvolution for pressure transient data interpretation and analysis had been an important challenge in the past because deconvolution is inherently an ill-conditioned inverse problem in the presence of noise in pressure and rate measurements. The deconvolution algorithms proposed in the past cannot tolerate typical levels of noise encountered in observed pressure and rate data in real applications.

In the pressure transient testing, each wellbore/reservoir system for a given time period, has a characteristic unit-impulse function (or response) denoted by $g(t)$, which is a time derivative of constant-unit-rate drawdown pressure response p_u(t) [i.e., $g(t) = dp_u(t)/dt$]. Besides, a common assumption in the pressure transient testing is made where if this system is governed by the pressure diffusion equation with a linear time-dependent inner boundary condition; its behavior is described by the linear convolution integral. In this case, (Everdingen and Hurst, 1949) stated the superposition principle holds and the relationship between the measured flow rate $q(t)$ and the measured pressure change $\Delta p = p_0 - p(t)$ is given by Duhamel's convolution integral:

$$\Delta p(t) = p_o - p(t) = \int_0^t g(t - t')g(t')dt', \quad (1.1)$$

where $p(t)$ is the measured wellbore pressure (the solution of the time-dependent boundary value problem for the forward problem), $po$is the initial reservoir pressure and $q(t)$ is measured in the wellbore or at the surface. Both $\Delta p$and Δq may contain measurement errors (noise) where usually the range is in between 0.01 to 5% for pressure and 1 to 15% for flow rates. This magnitude of noise could be differing significantly depending on the factors of measurement technology, wellbore environment and fluid.

Briefly, the purpose of deconvolution method is to estimate the unknown wellbore/reservoir unit impulse function,$g(t)$, and the constant-unit-rate drawdown pressure drop, $p_u(t)$ from equation (1.1) by using measured pressure $p(t)$ and flow rate $q(t)$. Solving the convolution integral (1.1) is known to be an ill-posed problem, mainly due to the violation of a solution stability condition and noise in $p(t)$ and $q(t)$.Hence, the solution approach needs additional information and constraints also special mathematical treatments to ensure stability and smoothness.

The new robust deconvolution method is developed by Pimonov et al. (2010) which based on the von Schroeter et al (2001, 2004), Levitan (2005) and Levitan et al. (2006), where this new algorithm is more comprehensive and used a total nonlinear least-squares method for performing pressure/rate deconvolution.

1.2 Problem Statement

In deconvolution algorithm, there are a few unknown algorithmic parameters including error levels in pressure and rate data, and the curvature constraint value as well as the initial pressure where these parameters will affect the results of deconvolved responses.

1.3 Objectives

- To analyze and interpret the effects of algorithmic parameters (including error levels in pressure and rate data, and the curvature constraint value) on the deconvolved responses.
- To analyze and interpret the effect of initial pressure on the deconvolved responses.
- To illustrate the effects of the algorithmic parameters on the deconvolved responses by using synthetic test data.

1.4 Scope of Study

This study involves a sensitivity study for the algorithmic parameters (including error levels in pressure and rate data, and the curvature constraint value) as well as the effects of initial pressure on the deconvolved responses. The sensitivity study will be conducted using the Pimonov et al. deconvolution algorithm and/or the ones implemented in Weatherford PanSystem Well Test Software. Then, a sensitivity study based on synthetic test examples will be conducted. The utility and importance of the deconvolution in pressure transient interpretation will be demonstrated on field examples.

Chapter 2

Literature Review

2.1 Deconvolution Concept and Basic

Over 50 years, deconvolution techniques have been applied for the well test analysis. Based on Gringarten (2008), deconvolution is not a new interpretation method, but a new tool to process pressure and rate data to obtain more pressure data to interpret. Besides, it is also used for the pressure transient analysis and interpretation. Deconvolution is a signal processing method in which the effect of time dependent input signal is filtered from the output signal as shown in the Figure 2.1 after Kuchuk et al. (2010). In the pressure transient testing, deconvolution could be defined as the determining the influences function or unit response behavior of a system (an equivalent constant-rate response), which is the equivalent constant-rate response from the measured transient pressure and flow-rate data.

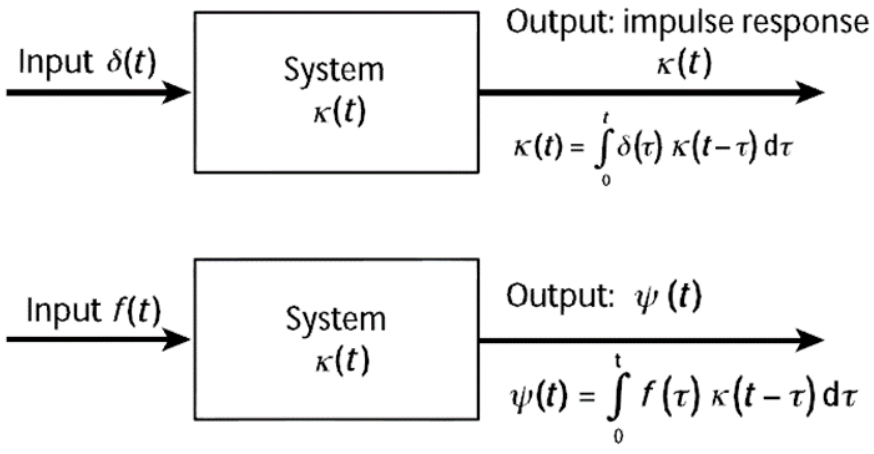

Figure 2.1: A Schematic representation of the deconvolution operation (Kuchuk et al. 2010).

The primary objective of applying deconvolution is to convert the pressure data response from a variable-rate test or production sequence into an equivalent pressure profile that would have been obtained if the well were produced at a constant rate for the entire duration of the production history. If such an objective could be achieved with some success, the deconvolved response would remove the constraints of conventional analysis techniques [D. Bourdet, et al. (1989); C.R. Earlougher (1977); D. Bourdet (2002)] that have been built around the idea of applying a special time transformation (e.g., the logarithmic multi-rate superposition time as suggested by R.G. Agarwal (1980)) to the test pressure data so that the pressure behavior observed during individual flow periods would be similar in some way to the constant-rate system response. In fact, the superposition-time transform does not completely remove all effects of previous rate variations and often complicates test analysis because of residual superposition effects, particularly if the late portions of the transients are influenced by reservoir boundaries.

Unfortunately, deconvolution requires the solution of an ill-posed problem which if there is a small changes in input (measured pressure and rate data) can lead to large changes in the output (deconvolved) result. Thus, this ill-posed nature of deconvolution problem combined with errors that inherent in pressure and rate data makes the application of deconvolution a huge challenge. Robust deconvolution algorithms is developed as remedy to this challenge where the algorithms are error-tolerant. A schematic illustration of p-r convolution and deconvolution problems of interest to pressure transient interpretation is shown in Figure2.2. Both problems uses the same superposition equation (1.1), but in a different manner as shown in Figure2.2.

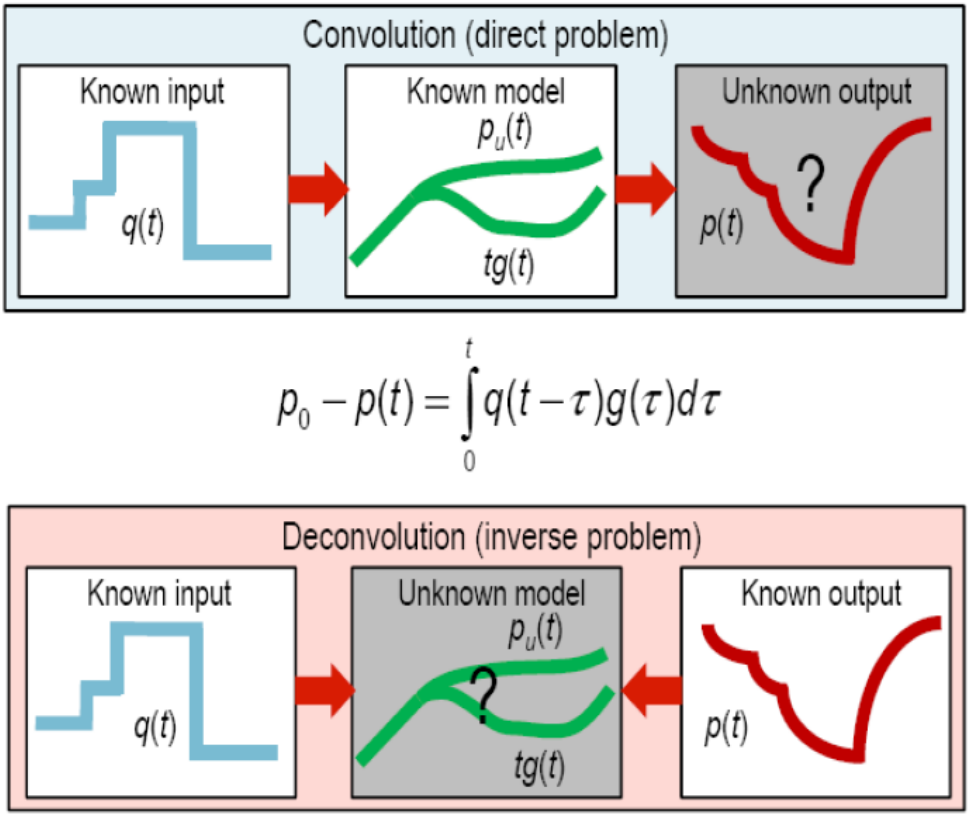

Figure 2.2: Pressure – rate convolution and deconvolution.

2.2 The Development of Deconvolution Algorithm

In the history of petroleum engineering literature, deconvolution method was not commonly used in the reservoir engineering problem until the 1980s but the developments of this method is started since 1959. Deconvolution firstly applied for determining the influences function directly from field data for aquifers [Hutchinson and Sikora (1959); Katz et al. (1962); Coats et al. (1964)]. In the 1965, Jargon and van Poollen (1965) applied deconvolution to compute the constant rate-pressure behavior which the influence function from transient pressure and rate data. Bostic, Agarwal and Carter (1980) have proposed another technique to obtain the influence function from variable rate and pressure history and in1981; Pascal (1981) has applied deconvolution to obtain constant-rate pressure measurements of a drawdown test. After 1981 there have been continuous

efforts to develop deconvolution techniques. [Kuchuk and Ayestaran (1985); Thompson et al. (1986); Gajdica et al. (1988); Kuchuk (1990); and Baygun (1997)] However, the methods cited above have their own hitches and had not been found successful to be implemented in any commercial software because these methods do not tolerate to acceptable noise levels commonly encountered in pressure and rate data.

Recently, the focus in the deconvolution has increased by introduction of more stable deconvolution algorithms by von Schroeter et al. (2001, 2002), and further extended or revised other authors subsequently. [Levitan (2005), Levitan et al (2006), Onur et al. (2008), Pimonov et al. (2008, 2009a, 2009b)] These algorithms have been incorporated in the most commercial well test analysis software because these algorithms have superior features over the previous deconvolution methods in terms of stability, error tolerant, etc. The development of deconvolution could be simply represented in Figure 2.3.

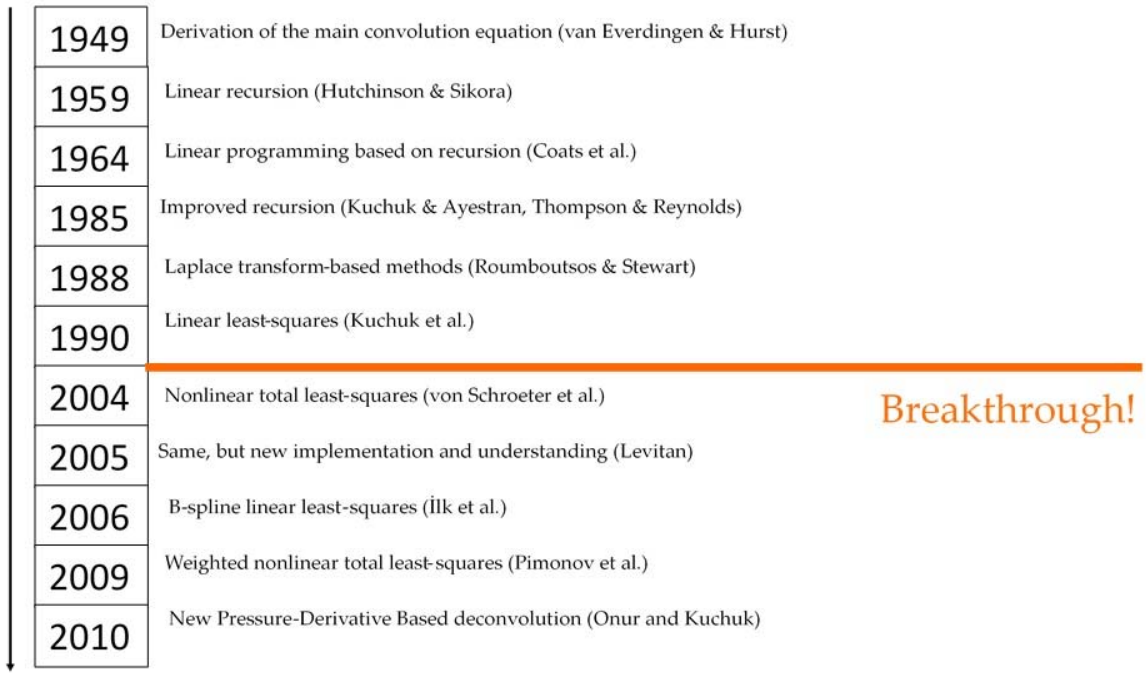

Figure 2.3: Timeline of deconvolution development in petroleum engineering literature.

Chapter 3

Methodology

3.1 Research Methodology Flow Chart

The Final Year Project (FYP) research on the analysis and interpretation of pressure transient test data by recent robust deconvolution methods begins with the literature review on the recent robust deconvolution methods [von Schroeter et al. (2001, 2004); Levitan (2005); Levitan et al. (2006); Ilk et al. (2005,2006); Onur (2008); Pimonov et al. (2008, 2009a, 2009b)] concept and nature. However Ilk et al. (2005, 2006) algorithm is excluded from this research because the Ilk et al. algorithm uses quadratic B-splines method with logarithmically distributed knots to represent the unknown $\boldsymbol{dp_u(t)/dt}$ where this algorithm has dissimilar nature compared to other recent robust deconvolution algorithms. Besides, Ilk et al. algorithm has the obvious disadvantages where the variable rate profile must be dissected into continuous segments and also its algorithm does allow for the estimation of initial pressure and rates.

In this research, by using and focusing on the recent robust deconvolution algorithm of Pimonov et al. and /or the ones implemented in Weatherford PanSystem Well Test Software, the effects of the algorithmic parameters (including error levels in pressure and rate data, and the curvature constraint value) as well as the initial pressure on the deconvolved responses are investigated. Several synthetic and field test data are used to illustrate the effects of the algorithmic parameters on the deconvolved responses as well as the importance of the deconvolution in analysis and interpretation of pressure transient data. The flow of the research methodology could be illustrated in Figure 3.1 as shown below.

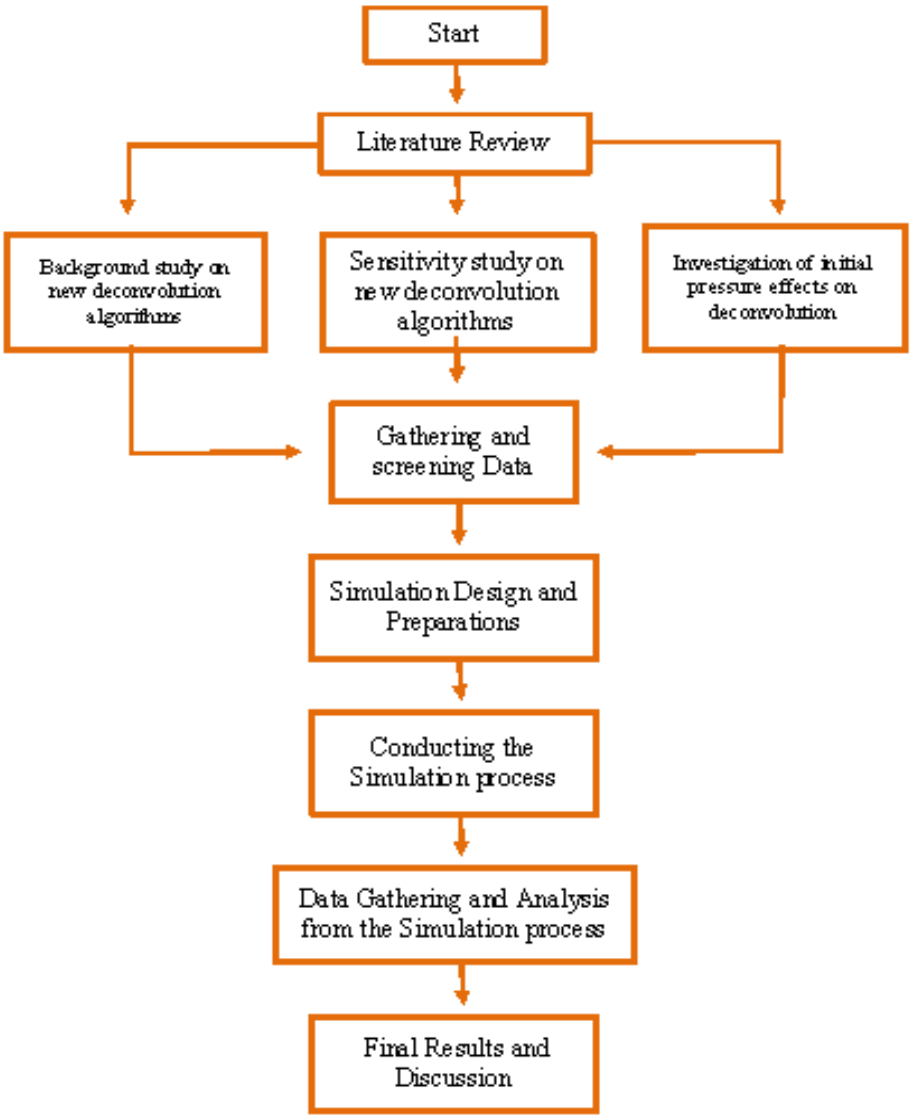

Figure 3.1: Flow chart on research methodology.

3.2 Project Gantt Charts

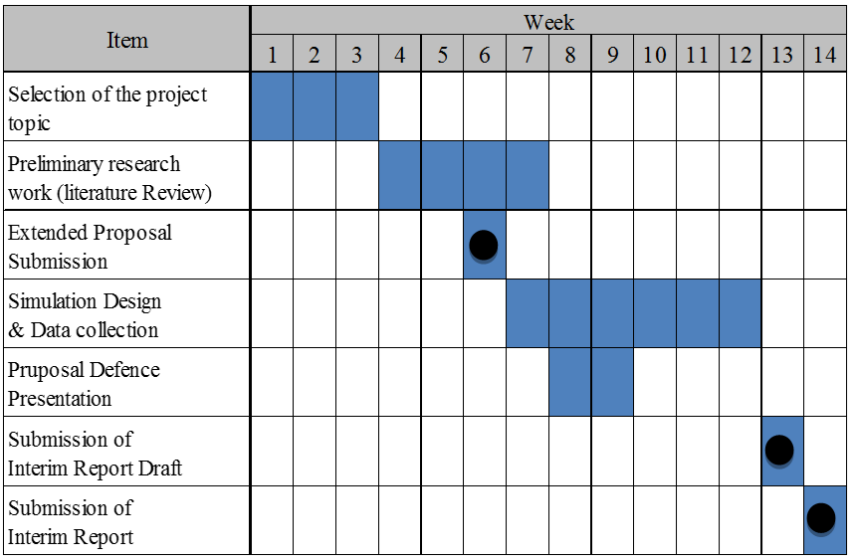

Figure 3.2: FYP 1 Gantt chart.

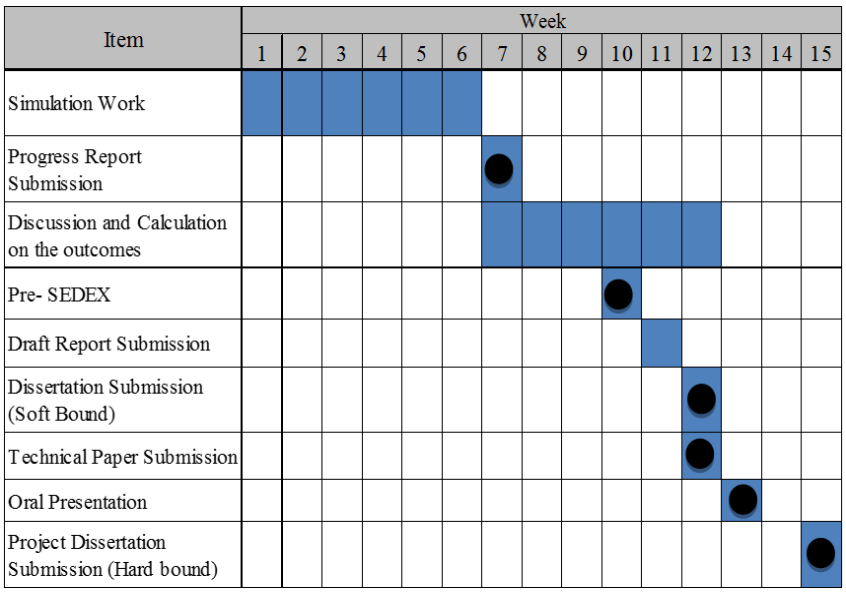

Figure 3.3: FYP 2 Gantt chart.

3.3 Software

Throughout this research, to conduct the sensitivity study on the recent robust deconvolution method including the effects of the algorithmic parameters (including error levels in pressure and rate data, and the curvature constraint value) as well as the initial pressure on the deconvolved responses; two software are being used which are one source code specific used for the deconvolution method which developed by Pimonov et al. (2010) and Weatherford PanSystem Well Test software.

3.1.1 Pimonov et al. (2010) codes

Pimonov et al. (2010) codes is developed by Pimonov et al. for the deconvolution method where it treats deconvolution as a nonlinear regression problem based on a Total Weighted Least Square (TWLS) objective function and also it gives the user option to perform the pressure-rate deconvolution. The objective function in Pimonov et al. deconvolution algorithm is defined by

$$E\left(z_1,\dots,z_N,q_1^u,\dots,q_{Nq}^u,p_o\right)=\frac{1}{2}\sum_{i=1}^{N_p}w_{p,i}^2\left(\frac{p_o-p_i-\Delta p_{model}\left(t_i,z_1,\dots,z_N,q_1^u,\dots,q_{Nq}^u\right)}{\sigma_p}\right)^2+$$

$$\frac{1}{2}\sum_{j=1}^{N_q}w_{q,j}^2\left(\frac{q_j-q_j^u}{\sigma_q}\right)^2+\frac{1}{2}\sum_{k=1}^{N-1}\left(\frac{\kappa_k(z_1,\dots,z_N)}{\sigma_c}\right)^2 \quad (3.1)$$

3.1.2 Weatherford PanSystem

In this research, version 3.5 of Weatherford PanSystem is being used. The Deconvolution module in PanSystem is based on work done at Imperial College, London, using the Total Least-Squares (TLS) method which introduced by von Schroeter et al., (2004). The user has control over the smoothness and rate optimization aspects of the process, and can therefore make repeated runs until satisfied with the results. The objective function implemented in the von Schroeter et al. deconvolution algorithm is defined by

$$E(p_o,\boldsymbol{z},\boldsymbol{y})=\|p_o\boldsymbol{e}-\boldsymbol{p}_m-\boldsymbol{C}(\boldsymbol{z})\boldsymbol{y}\|_2^2+\upsilon\|\boldsymbol{y}-\boldsymbol{q_m}\|_2^2+\lambda\|\boldsymbol{D}\boldsymbol{z}-\boldsymbol{k}\|_2^2 \quad (3.2)$$

Chapter 4

Results and Discussion

4.1 Sensitivity Study Using Simulated Data

To test the proposed recent robust deconvolution algorithm (Pimonov et al.), two synthetic (simulated) test examples are considered. The examples are defined as follows:

- A simulated well test example of the Pimonov et al. (2010) where by taking consideration of different number of nodes is modeled for the deconvolved pressure response by using Pimonov et al. codes.
- A simulated well test example by using Weatherford PanSystem Well Test Analysis Software which implemented the Total Least Square (TLS) method; is modeled for deconvolved pressure response by taking consideration of different number of nodes and optimization of flow rates.

4.1.1 Synthetic Example 1

This is a well test performed on an oil well which the total test duration is 350 hours. The well/reservoir model is a fully penetrating vertical well in a closed rectangular reservoir with all boundaries being no-flow. The reservoir is 4000 ft. long and 1500 ft. wide as shown in Figure 4.1. Pressure and rate data for this simulated test example are shown in Figure 4.1 and Figure 4.2, respectively. The test data include three pressure drawdown periods and single pressure buildup period. In this synthetic example, the pressure and rate data are free of errors. Using the rate data and only the pressure data pertaining to only the buildup portion were used to reconstruct the unit-rate drawdown response. Nine different values of the number of nodes for deconvolution, from 20 nodes up to 100 nodes were used to reconstruct the unit-rate response and to investigate whether the unit-rate

response show sensitivity to the number of nodes used in deconvolution. The input parameters are given in Table 4.1.

The number of nodes used in the deconvolution can affect the quality of the deconvolved derivative in terms of coarseness. Therefore, the objective here is to test the performance of Pimonov et al. algorithm for this in consistent data set.

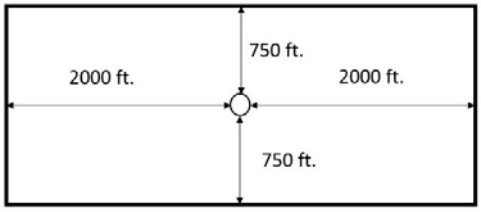

Figure 4.1: **Reservoir/well configuration for synthetic example**.

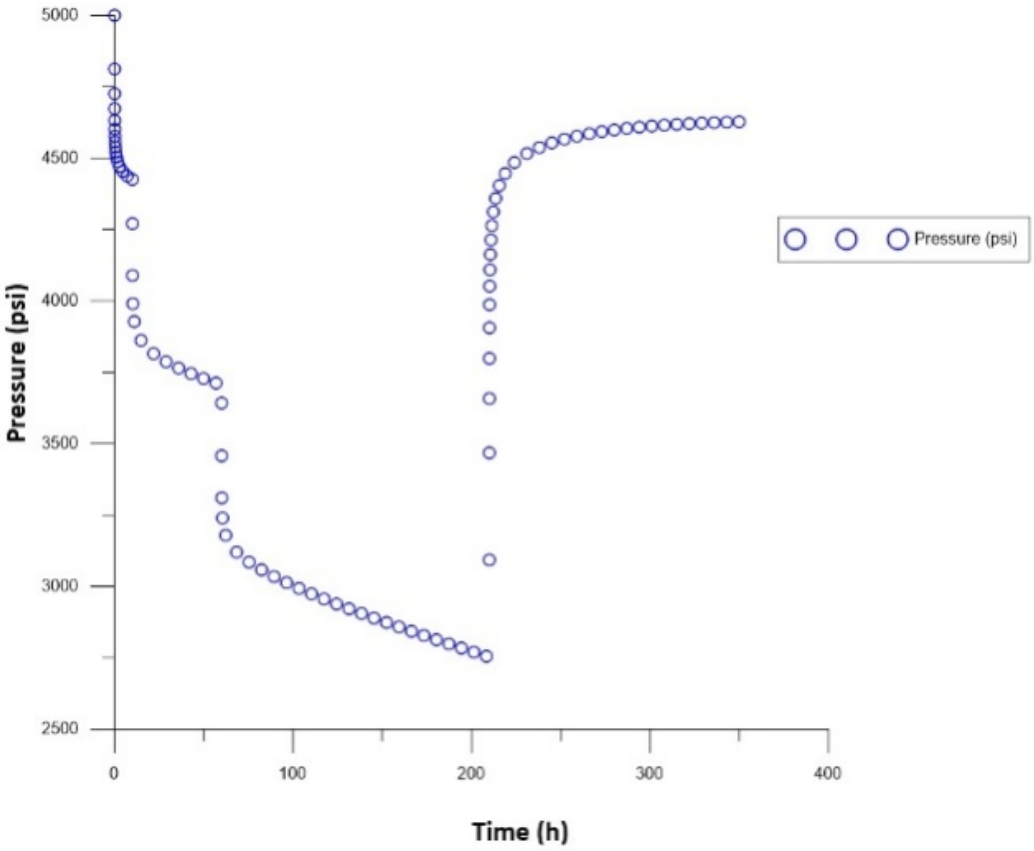

Figure 4.2: Pressure data for Synthetic Example 1

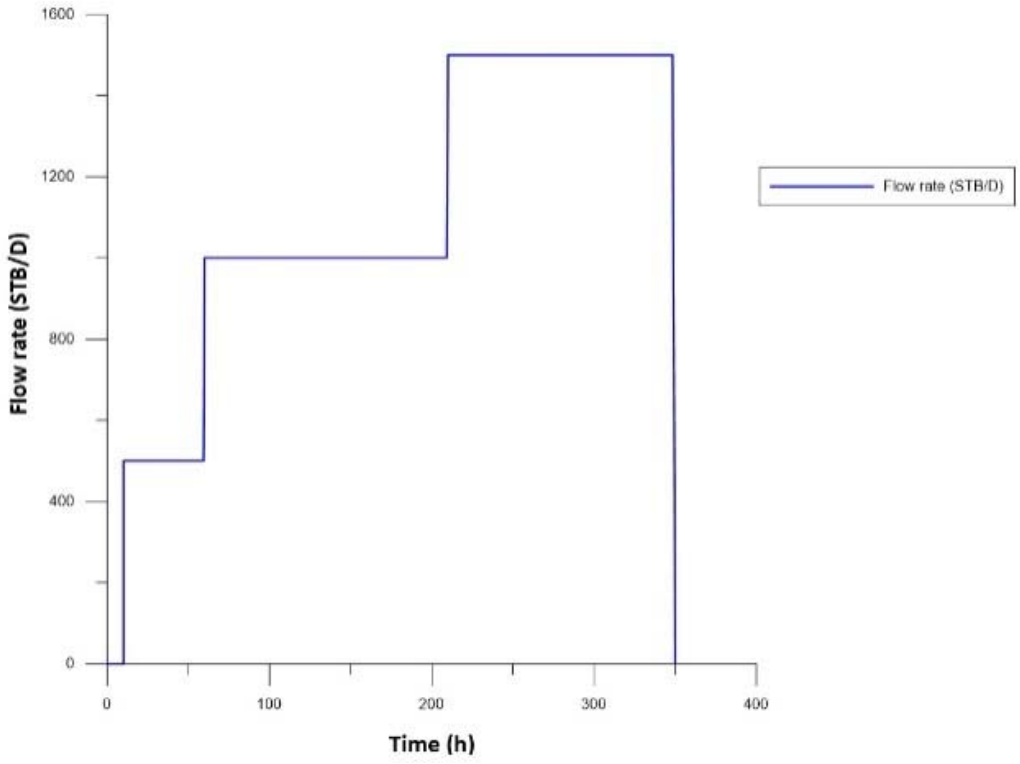

Figure 4.3: Rate data for the Synthetic Example 1

TABLE 4.1 – INPUT PARAMETERS FOR SYNTHETIC EXAMPLE 1 AND EXAMPLE 2	
∅, fraction	0.10
$\boldsymbol{h}$, ft	30
$\boldsymbol{c_t}$, psi^{-1}	$\mathbf{1.0 \times 10^{-5}}$
$\boldsymbol{\mu}$, cp	1.0
$\boldsymbol{r_w}$, ft	0.25
S, dimensionless	1.0
$\boldsymbol{p_i}$, psi	5000

Figure 4.4 present the comparisons of results of deconvolution obtained by using the buildup pressure data sets by processing with different number of nodes which begin with the 20, 30, 40, 50, 60, 70, 80, 90 and 100 number of nodes. For each number of nodes investigated, the flow rates and initial pressure are fixed. The recommended default values of the other required parameters for the Pimonov et al. algorithm is used.

Based on the Figure 4.4, each number of nodes gives almost identical results for the $\boldsymbol{p_u(t)}$ function and its natural logarithmic derivative for the buildup period. By comparing the deconvolved pressure response result generated by the Pimonov et al. algorithm with the true test pressure model, the optimum number of nodes for the Pimonov et al. algorithm could be concluded as 40 nodes. At this stage, by using 40 number of nodes, this deconvolution algorithm could generate the deconvolved pressure response which approximately identical with pressure response model and this is present in Figure 4.5.

Besides, these results verify that the Pimonov et al. algorithm can be applied to individual flow periods and this algorithm could be used on inconsistent data sets for which the initial reservoir pressure and flow rates are exactly known.

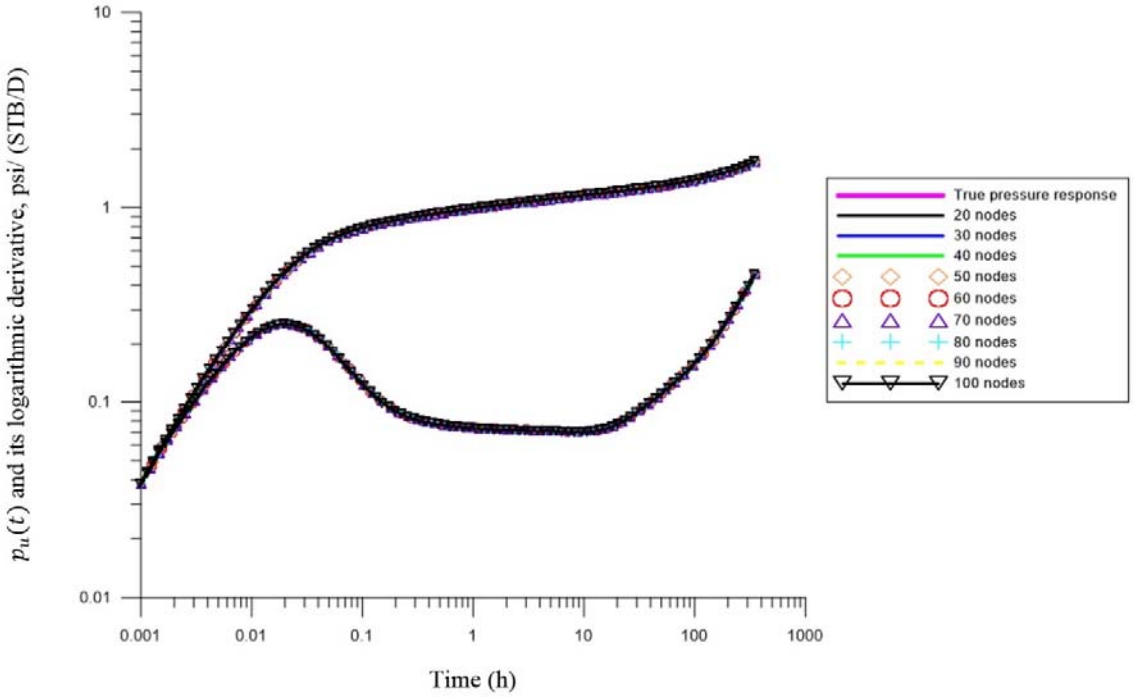

Figure 4.4: **The pressure responses obtained by deconvolution of the buildup period; Synthetic Example 1.**

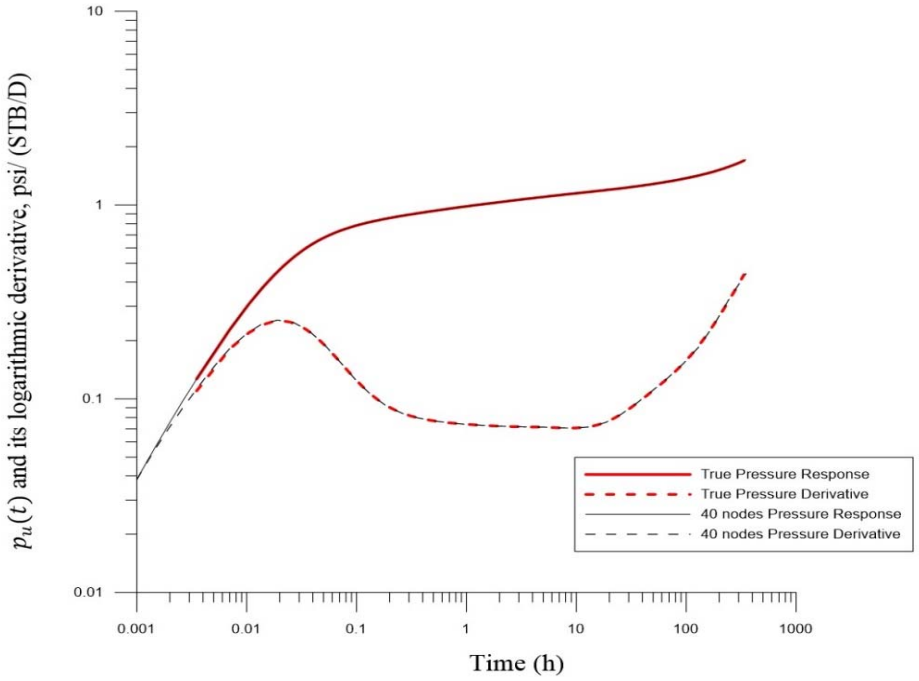

Figure 4.5: Comparison between true and 40 nodes of Pimonov et al. models.

4.1.2 Synthetic Example 2

For this synthetic example, the same pressure and rate test data for Synthetic Example 1 will be used where the test data are free from errors. In this investigation, we also consider pressure data only for build portion. Besides, the investigation is conducted by using Weatherford PanSystem version 3.5 where its deconvolution algorithm is based on the Total Least Square (TLS) method which is introduced by von Schroeter et al. (2004) and five different number of nodes begin with 15, 25, 40, 60 and 70 number of nodes are used throughout the investigation.

Regularization is used in this test by taking a constant value of $\boldsymbol{\lambda}$ throughout the test ($\boldsymbol{\lambda = 6.08785 \times 10^{5}}$) where this regularization parameter acts as the derivative smoothness term in the TLS method. Also, in this synthetic example, two tests are conducted to investigate the effect of number of nodes towards the deconvolved pressure response by optimization and de-optimization of the flow rates. Flow rates optimization contains the weighting value of $\boldsymbol{v}$ for the optimization of the rate term in the TLS method. For the first test, flow rates are not be optimized by set the value of $\boldsymbol{v = 0}$ and the flow rates will not be modified. For the second test, the flow rates is optimized by set the value of $\boldsymbol{v = 2.7057 \times 10^{-1}}$.

Figure 4.6 and Figure 4.7 present of the results of deconvolution obtained from the different number of nodes (from 15 to 70) for the pressure build up data set by processing them separately with the optimized and non-optimized flow rates option. For each number of nodes investigation, initial pressure is fixed and the recommended default values of the required parameters for the von Schroeter et al. algorithm are used.

Both figure shown that the optimize flow rates give almost identical result for the $\boldsymbol{p_u(t)}$ function and its natural logarithmic derivative for the buildup period but the number of nodes do affect the deconvolution results which the lowest number of nodes (15 nodes) give low quality and coarse pressure response signal. As mentioned earlier, the number of nodes affect the quality of the deconvolved derivative in terms of smoothness; therefore, the higher number of nodes will give the good quality of deconvolved derivative and in this example, the optimum number of nodes of the von Schroeter et al. algorithm implemented in Weatherford PanSystem is 70.

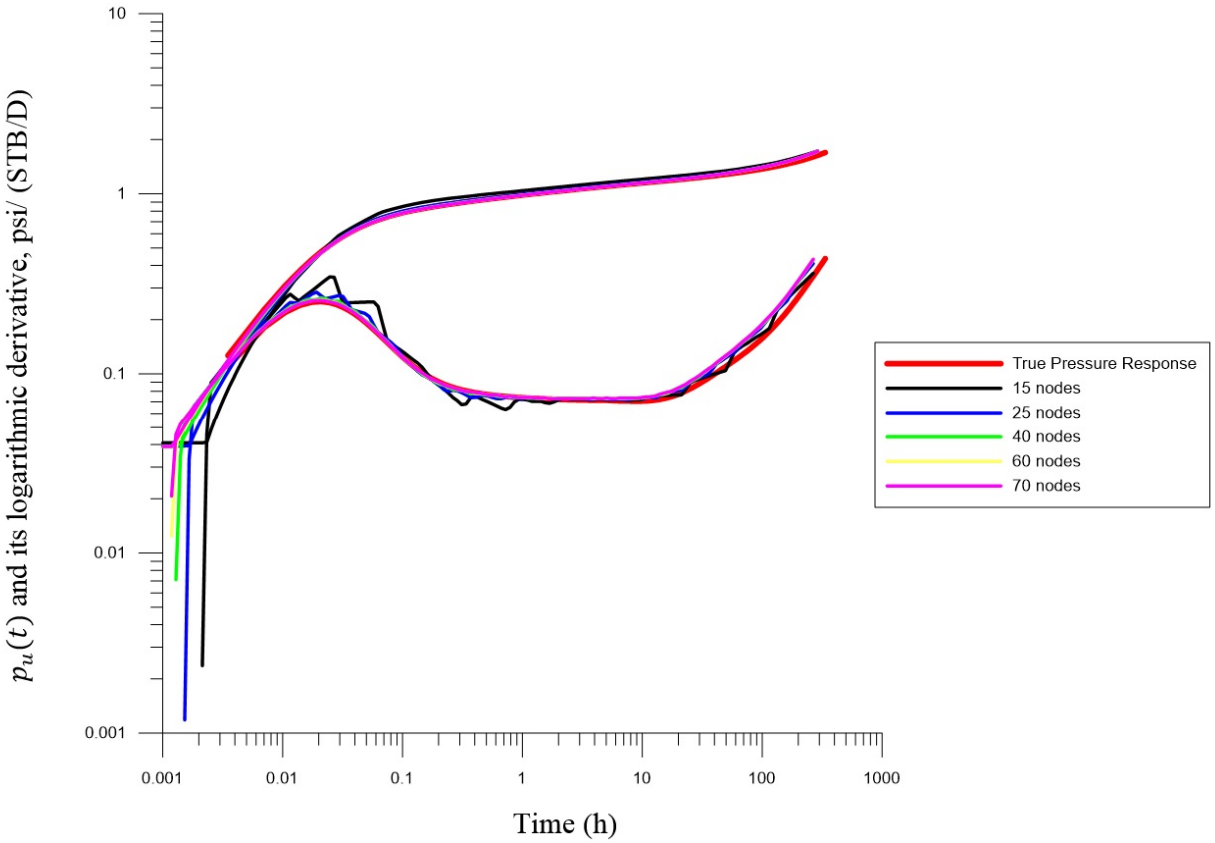

Figure 4.6: The pressure responses obtained by deconvolution of the buildup period without optimize flow rates; Synthetic Example 2

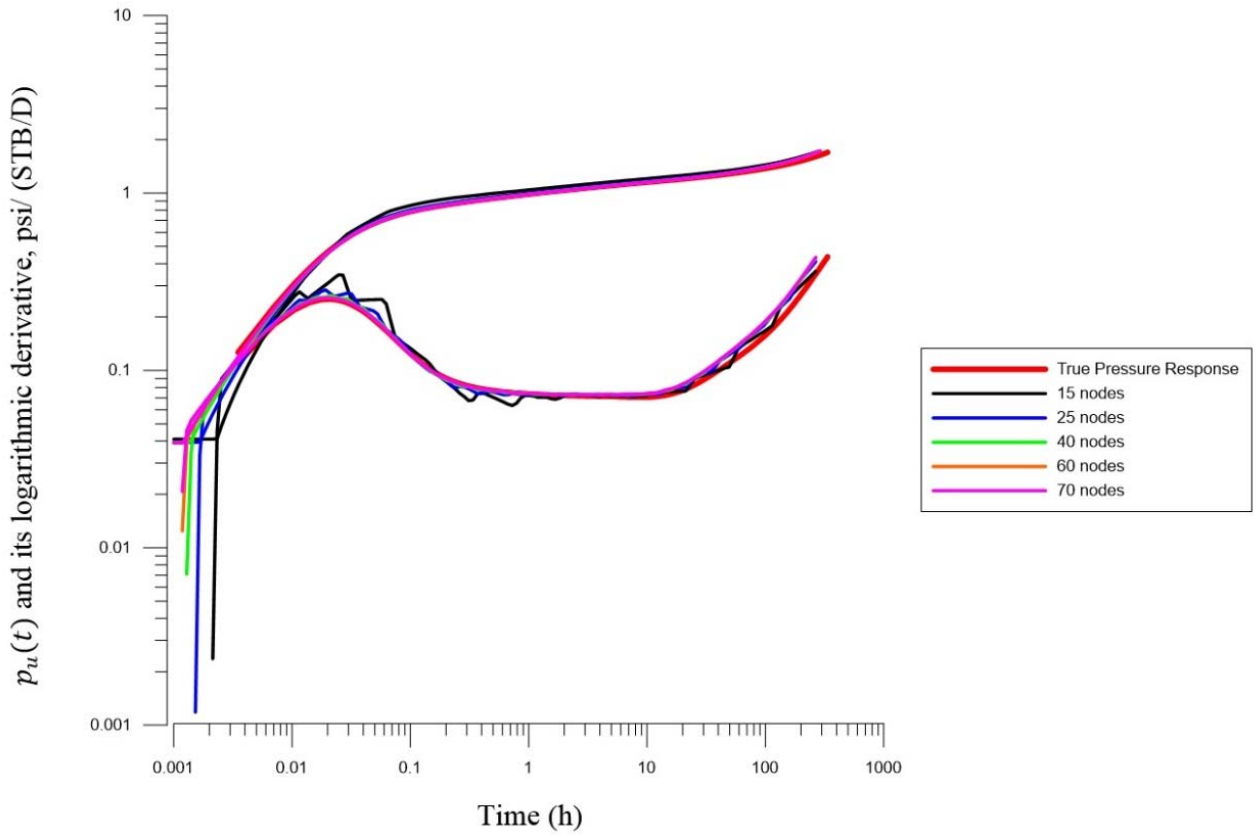

Figure 4.7: The pressure responses obtained by deconvolution of the buildup period with optimize flow rates; Synthetic Example 2

By comparing the deconvolved pressure response result generated by the Weatherford PanSystem with the true test pressure model, the optimum number of nodes of 70 still insufficient to consider as approximately identical compared to the Pimonov et al. codes which has optimum number of nodes of 40 and this could be presented in Figure 4.8. Although Weatherford PanSystem do give slightly low quality of deconvolved derivative results compared to Pimonov et al. codes, the results from the synthetic example 2 verify that the Weatherford PanSystem can be applied to individual flow periods and the von Schroeter et al. algorithm implemented in Weatherford Pansystem could be used on inconsistent data sets for which the initial reservoir pressure and flow rates are exactly known.

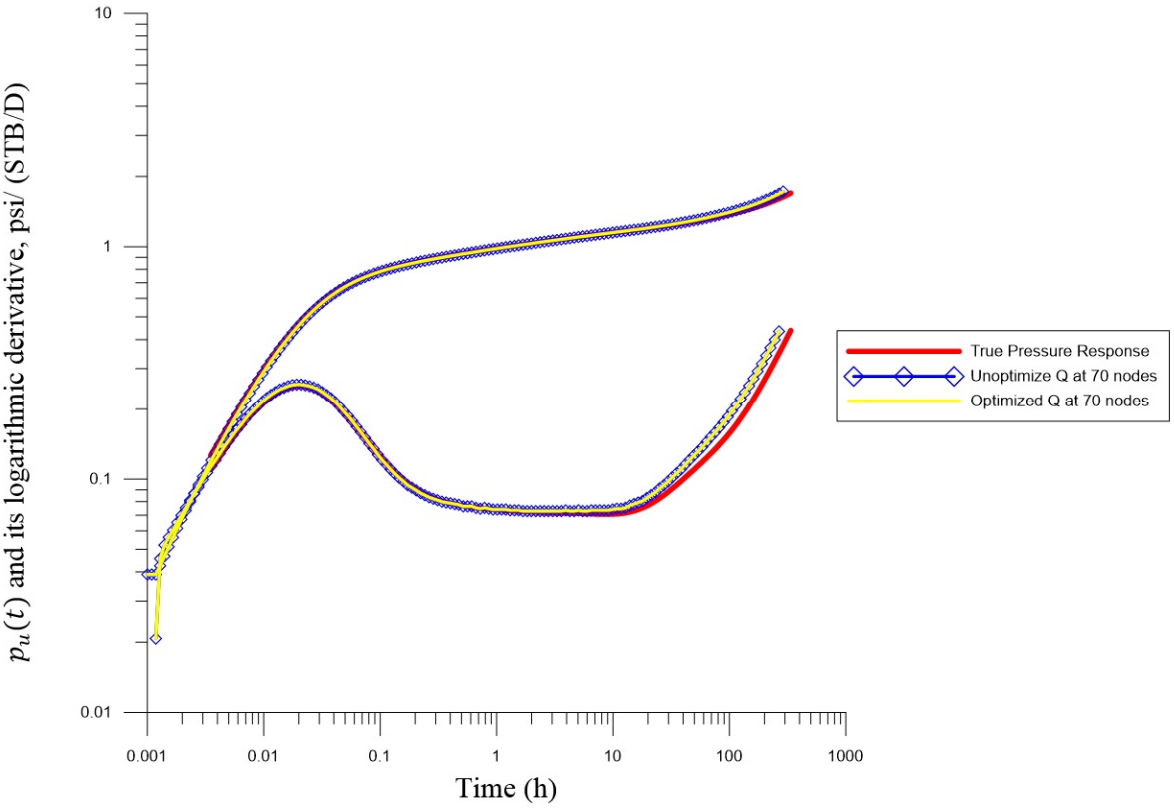

Figure 4.8: Comparison between true and 40 nodes of Weatherford PanSystem models.

4.1.3 Synthetic Example 3

This synthetic example is presents the investigation on the effects of the error efficiency level (η_p and η_q) towards the deconvolved response and compared with the true deconvolved response. The true pressure and rate data used is consists of two buildup periods and two drawdown periods as illustrated in Figure 4.9 and Figure 4.10. In this example, a fractured vertical well with infinite conductivity and rectangular closed system boundaries with dimensions of 4000 ft. long and 2000 ft. wide could be presented by Figure 4.11. The reservoir input parameters are given in Table 4.2.

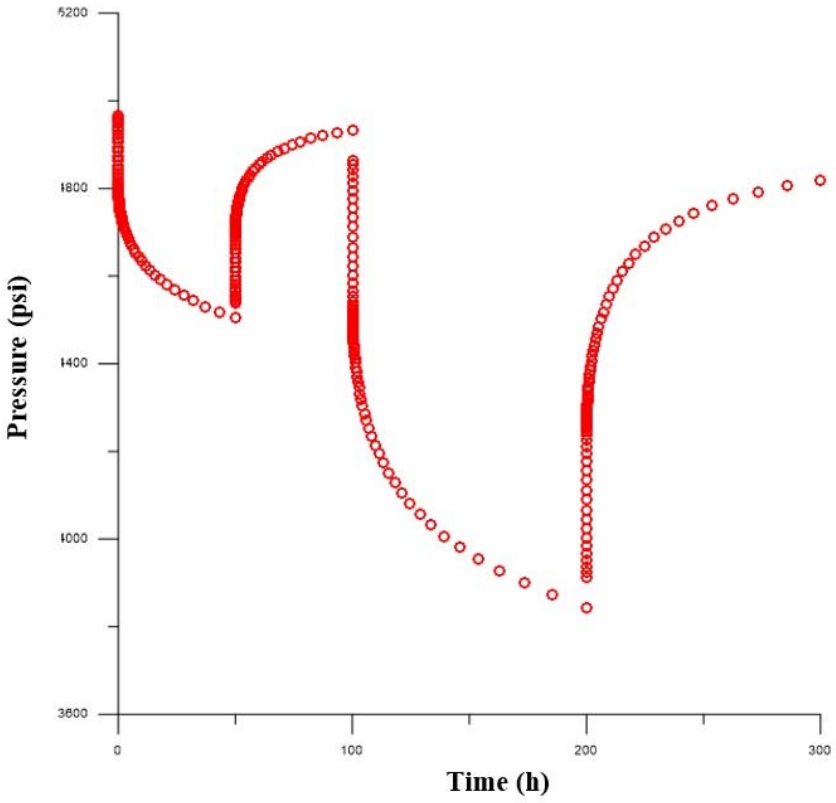

Figure 4.9: Pressure data for Synthetic Example 3

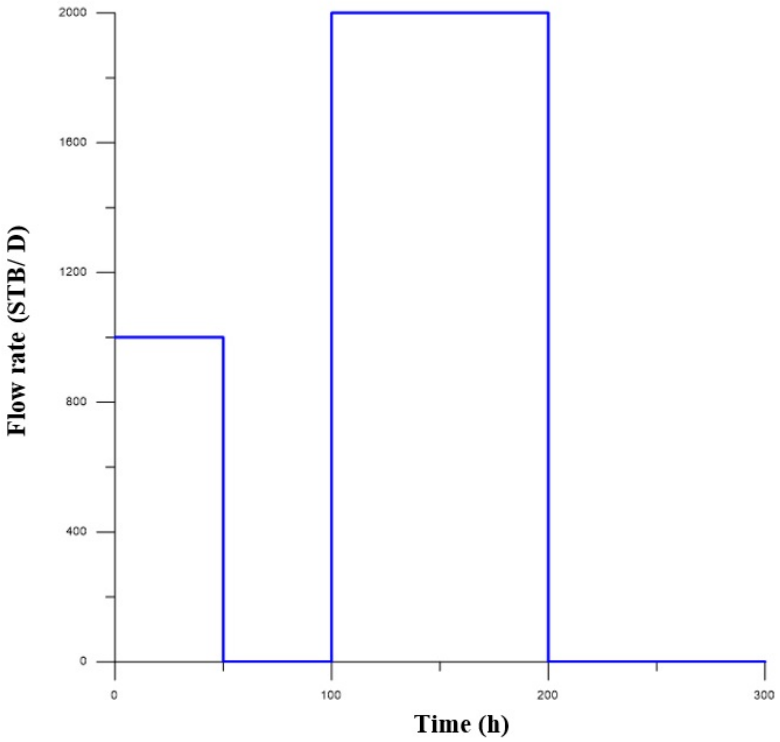

Figure 4.10: Rate data for Synthetic Example 3

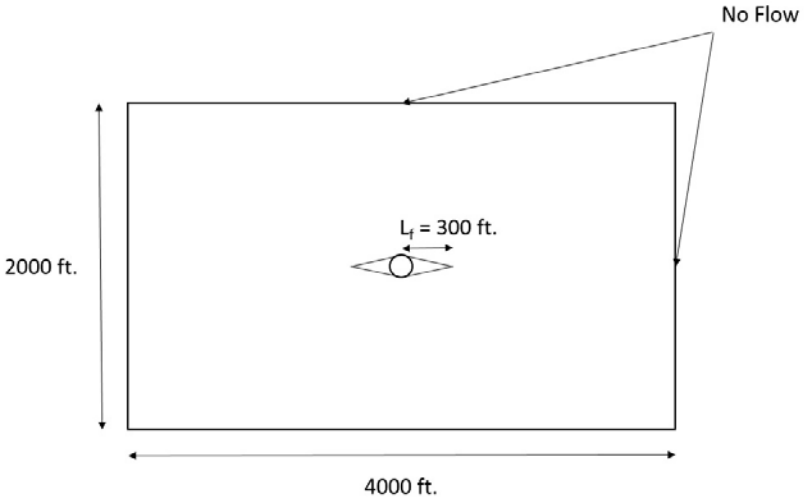

Figure 4.11: Reservoir geometry for Synthetic Example 3

TABLE 4.2 – INPUT PARAMETERS FOR SYNTHETIC EXAMPLE 3	
∅, fraction	0.20
$\boldsymbol{h}$, ft	35
$\boldsymbol{c_t}$, psi^{-1}	1.0×10^{-5}
$\boldsymbol{\mu}$, cp	0.5
$\boldsymbol{r_w}$, ft	0.3
$\boldsymbol{C_w}$, bbl/psi	0.001
$\boldsymbol{S}$, dimensionless	1.0
$\boldsymbol{L_f}$, ft	300
$\boldsymbol{p_i}$, psi	5000
$\boldsymbol{k}$, md	10
$\boldsymbol{B_o}$, RB/STB	1

Figure 4.9 and figure 4.10 present the true pressure and flow rate data run for 300 hours duration. For this example, the true data (pressure and flow rate) is corrupted by introducing specific level of noise in the data which known as error level efficiency (η_p and η_q). There are five cases with different error level efficiency is investigated as tabulated in Table 4.3 and for this example, the test is run by using whole periods of data for deconvolution.

Initially, a 1 % of error level efficiency is introduced for pressure and flow rate with zero mean and standard deviation of 5.0595 psi and 11.1803 B/D is added to pressure and rate data respectively to corrupt the data. The pressure and flow rate data which containing noise is illustrated in Figure 4.12 and Figure 4.13 respectively. The error efficiency level has significant relationship with the pressure and flow rate data as well as the standard deviation (error level which represents by σ_p, σ_q, and σ_c). Besides, the relationship

between pressure and rate error efficiency and error levels (σ_p and σ_q) is investigated respectively based on the following equations (von Schroeter et al., 2002; 2004):

$$\sigma_p = \frac{\eta_p \|\Delta \boldsymbol{p}\|_2}{\sqrt{M}}$$

$$\sigma_q = \frac{\eta_q \|\boldsymbol{q}\|_2}{\sqrt{N}}$$

The curvature constraint, σ_c value is set as constant at the value of 0.05 throughout the test.

Table 4.3: Deconvolution parameters used for the synthetic example 3 (Pimonov et al. algorithm)

Case	η_p (percentage)	η_q (percentage)	σ_p (psi)	σ_q (B/D)	σ_c (unitless)
Case 1	1.00	1.00	5.0595	11.1803	0.05
Case 2	1.00	10.00	5.0595	111.8034	0.05
Case 3	5.00	10.00	25.2977	111.8034	0.05
Case 4	5.00	15.00	25.2977	167.7051	0.05
Case 5	5.00	20.00	25.2977	223.6068	0.05

Pimonov et al. (2009b) algorithm is applied in this example to process the pressure data for the whole test sequence in one pass with the initial pressure of 5000 psi. For the first task, Pimonov et al. algorithm is used to process the whole five cases with different values of error level and compared with the true pressure response. Figure 4.14 presents the true pressure unit response and true pressure logarithmic derivative curve.

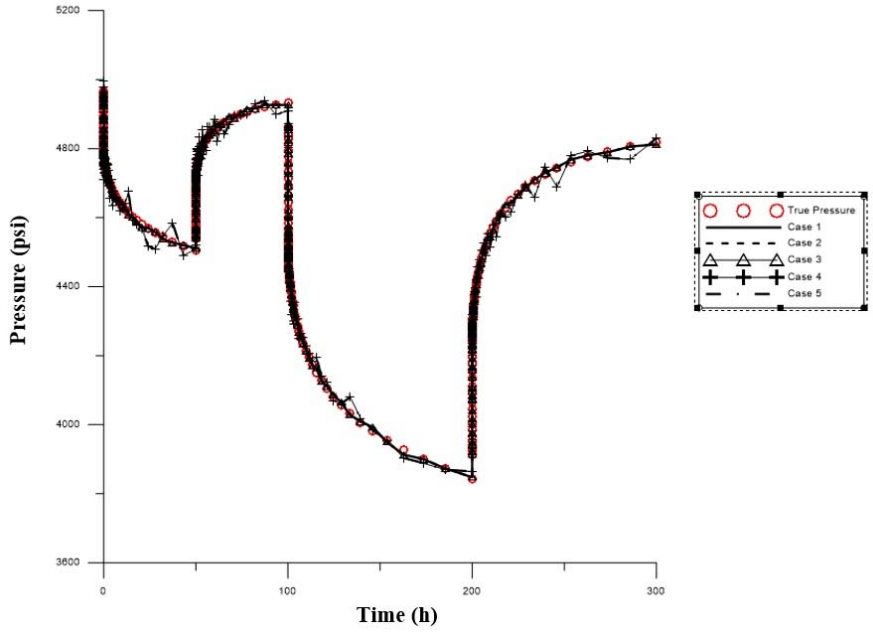

Figure 4.12: True pressure history and corrupted pressure history (contains noise)

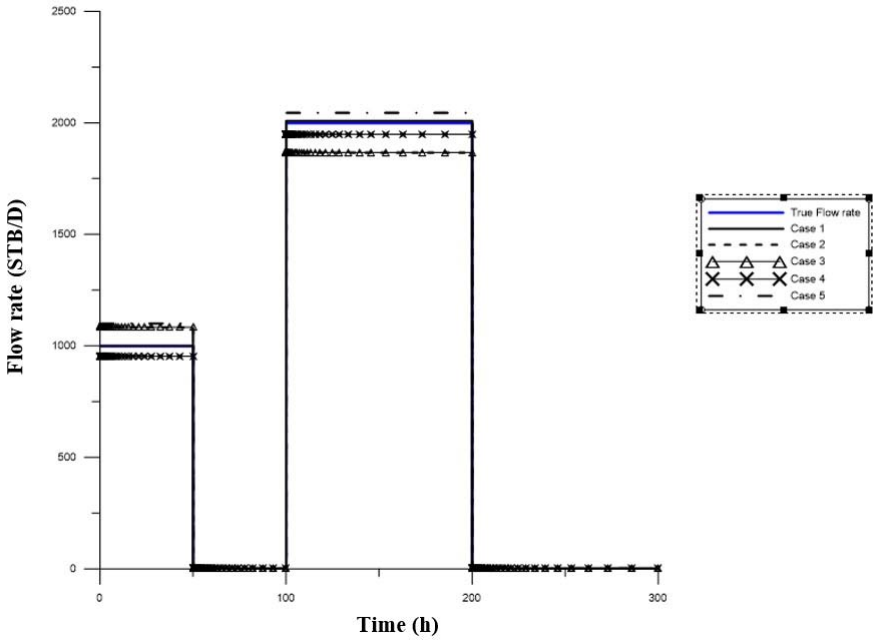

Figure 4.13: True flow rate history and corrupted flow rate history (contains noise)

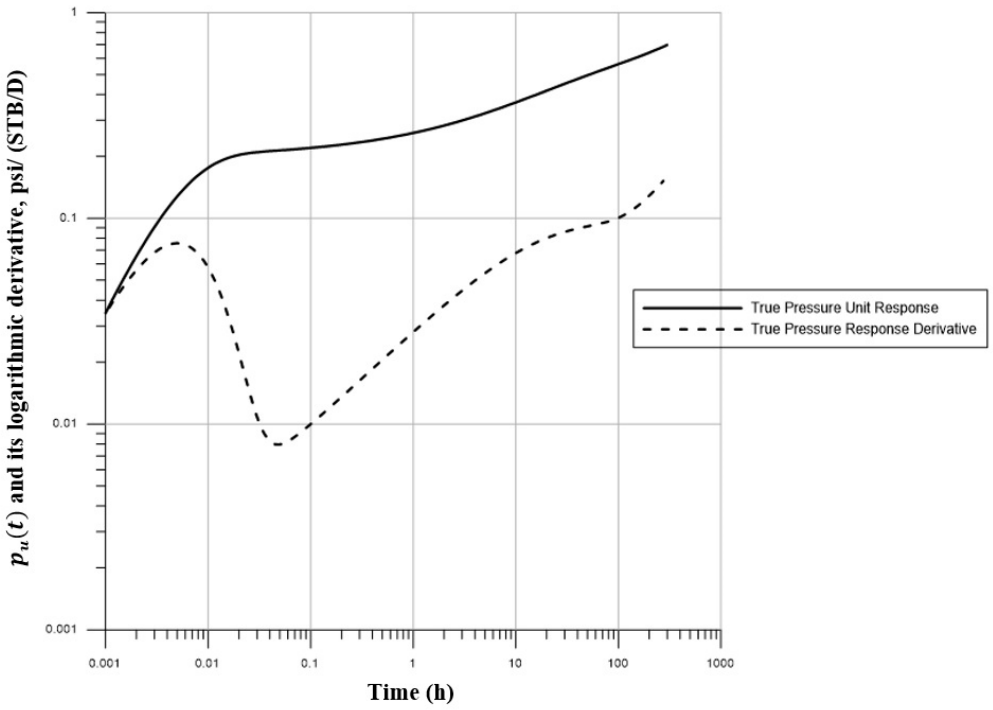

Figure 4.14: True pressure unit response and its derivatives

Based on figure 4.14 above, in early time region of this fractured vertical well with infinite conductivity, true pressure response derivative shows a smooth fluctuation movement from 0.001 to 0.1 hours, perhaps this is due to the wellbore storage effect or dynamics of fluid movement in the wellbore during which measurement uncertainties are high and also skin effect is taking into consideration. Starting on 0.1 to 10 hours the reservoir is having fractured linear flow towards the wellbore and this is interpreted based on the ½ slope of the pressure derivative slope. A transition from fractured linear flow to late radial flow could be seen at the late time region from 10 to 100 hours and at 100 hours onwards, the flow has reach reservoir boundary and having reservoir boundary effect where this indicates by 1 unit slope.

The comparison between five proposed cases with the true pressure response is shown in the Figure 4.15 where all the cases are smooth approximately match the true response and the only constraint is the signal fluctuations are seen in the early time region from 0.001 to 0.1 hours. At this stage, only pressure unit response from Case 1 and Case 2 is approximately match the true unit response, perhaps this is due to the presence of low error level (noise) in the data. Besides, other cases (Case 3, 4 and 5) deviated from the true unit response in the early time region and mismatch the true unit response but all the pressure unit response generated from each cases successfully to match approximately the true unit response starting from 1 hours onwards.

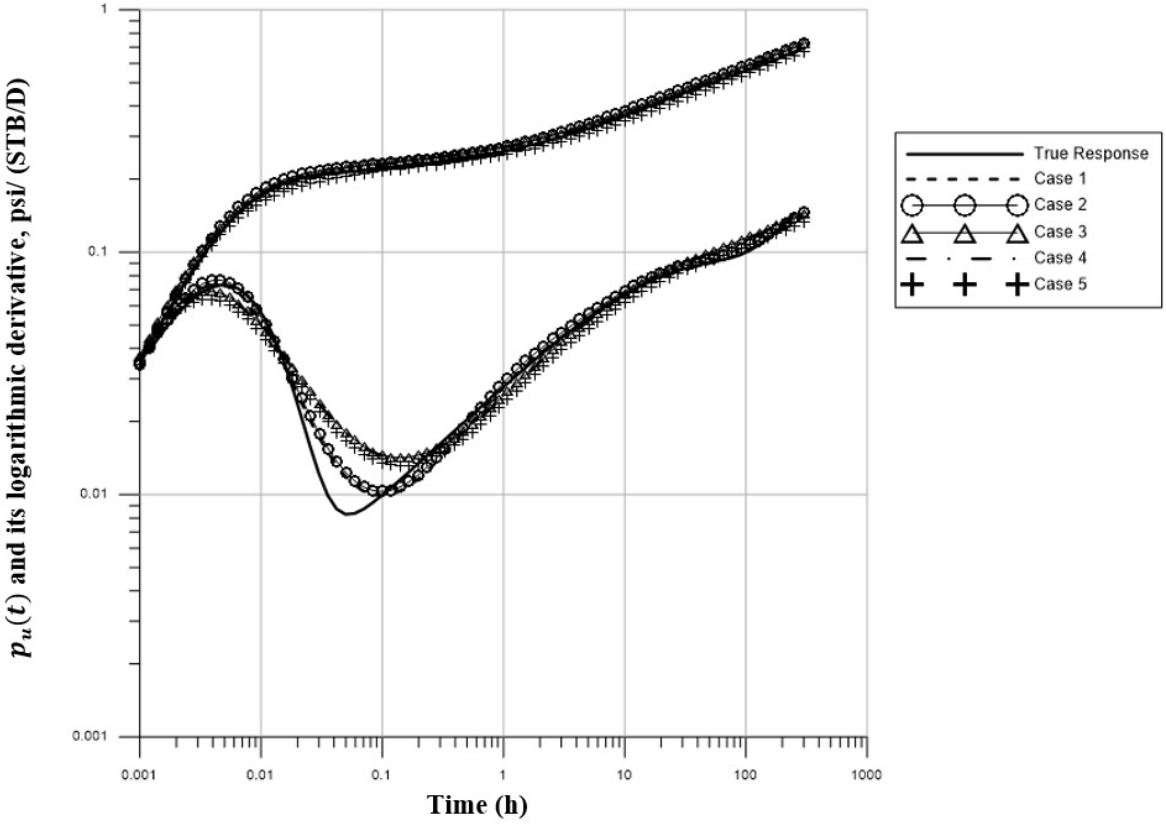

Figure 4.15: Comparison of deconvolution responses and derivatives with true and five different cases of parameters given in Table 4.3 for synthetic example 3.

The reason of fluctuation in the early time region may because of the presence of error level (σ_p and σ_q) in the pressure and rate data where leads to the poor approximation of a reservoir model which having wellbore storage and skin effects. Based on this comparison study, Pimonov et al. algorithm could generate a good unit response signal for pressure and rate data from the field but at a certain level of noise. In this study showing that the best percentage of error that could be handle by Pimonov et al. algorithm to receive a better output is 1 and 10 % of error in pressure and error data respectively and this could be presented by Case 1 and Case 2.

Further study is conducted for this synthetic example 3 is to apply the von Schroeter et al. deconvolution algorithm which implemented in the Weatherford Pan System software to process the corrupted data (data with noise) of pressure and rate in the algorithm. The same approach is taken as the first task to compute the deconvolution algorithmic parameters σ_p, σ_q, and σ_c by based on the error efficiency percentage. The initial pressure is set to 5000 psi and consider 75 uniform logarithmically spaced nodes for the z_d response.

Furthermore, the values of the parameters υ and λ could be related to the average variances of pressure, $(\sigma_p)^2$ and rate, $(\sigma_q)^2$ data, and the curvature constraint,$(\sigma_c)^2$ by the following equations (Onur et al., 2008):

$$\upsilon = \frac{\sigma_p^2}{\sigma_q^2}$$

$$\lambda = \frac{\sigma_p^2}{\sigma_c^2}$$

Using the above equations, and fixed value of $\sigma_c^2 = 0.0025$, the values of the parameters υ and λ for each error efficiency percentage could be computed and tabulated in Table 4.4.

Table 4.4: Deconvolution parameters used for the synthetic example 3 (von Schroeter et al. algorithm)

Case	η_p (percentage)	η_q (percentage)	υ (psi D/B)	λ (psi^2)	σ_p^2 (psi^2)	σ_q^2 ((B/D)^2)	σ_c^2 (unitless)
Case 1	1.00	1.00	0.2048	10239.59	25.5990	125	0.0025
Case 2	1.00	10.00	0.0020	10239.59	25.5990	12500	0.0025
Case 3	5.00	10.00	0.0512	255989.7	639.9744	12500	0.0025
Case 4	5.00	15.00	0.0228	255989.7	639.9744	28125	0.0025
Case 5	5.00	20.00	0.0128	255989.7	639.9744	50000	0.0025

In this task, full test sequence is being processed by using von Schroeter et al. (2004) algorithm which implemented in the Weatherford Pan System software with the initial pressure of 5000 psi and the results of the deconvolution obtained based on deconvolution parameters in Table 4.4 is illustrated in Figure 4.16.

As shown in Figure 4.16, the von Schroeter et al. algorithm is less tolerant with noise level in the pressure and rate data which leads the deconvolved response from each cases is fluctuates rigorously especially in the early time region. The fluctuation problem which occurs in the early time region (also experienced by Pimonov et al. algorithm) perhaps due to the wellbore storage and skin effects; also with noisy data, von Schroeter et al. algorithm could not generate a smooth pressure unit response for identification of reservoir model. Besides, the rigorous fluctuation of unit response signals disturb the analysis and interpretation of flow regime in the reservoir either in the early, middle or late time region.

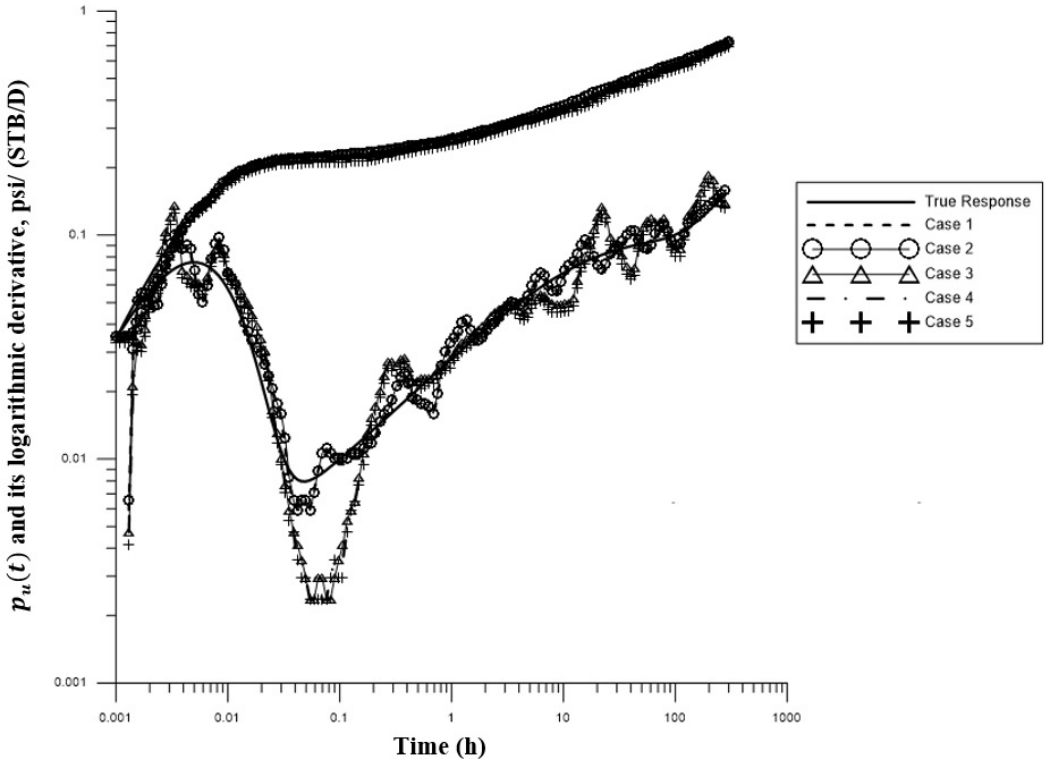

Figure 4.16: Comparison of deconvolution responses and derivatives with true and five different cases of parameters given in Table 4.4 for synthetic example 3.

Based on this study, again Case 1 and Case 2 could be considered as the best result compared to the other cases because the unit response signals generated from these two cases are approximately match the true pressure response even the signals are fluctuate. For von Schroeter et al. algorithm, in order to obtain a good deconvolved response as an output, the maximum error percentage in the pressure and rate data need to be set at 1 and 10 % respectively. If error percentage in the pressure and rate data exceed these two values, a bad output will be obtained with deconvolved response fluctuates severely.

By comparing the deconvolved response given by Pimonov et al. and von Schroeter et al. algorithms, Pimonov et al. algorithm is given more promising output for analysis and identification of reservoir model even with higher percentage of error efficiency. As

shown in Figure 4.16, all the five cases responses and derivatives' behave differently and more fluctuates especially in the early time region for von Schroeter et al. algorithm compared to the Pimonov et al. algorithm as shown in Figure 4.15. Based on analysis of both algorithms, it is shows that both algorithms (Pimonov et al. and von Schroeter et al.) have certain level of acceptable value for error level efficiency in pressure – rate data and the most promising algorithm and also error tolerant is the Pimonov et al. algorithm.

4.1.4 Synthetic Example 4

In this synthetic example, a deconvolution example is presents from an infinite conductivity vertical fractured well in a rectangular closed system boundaries (no-flow) reservoir with a dimension of 2000 ft. × 2000ft. as shown in the figure below. Besides, the formation and fluid properties data are tabulated in Table 4.5.

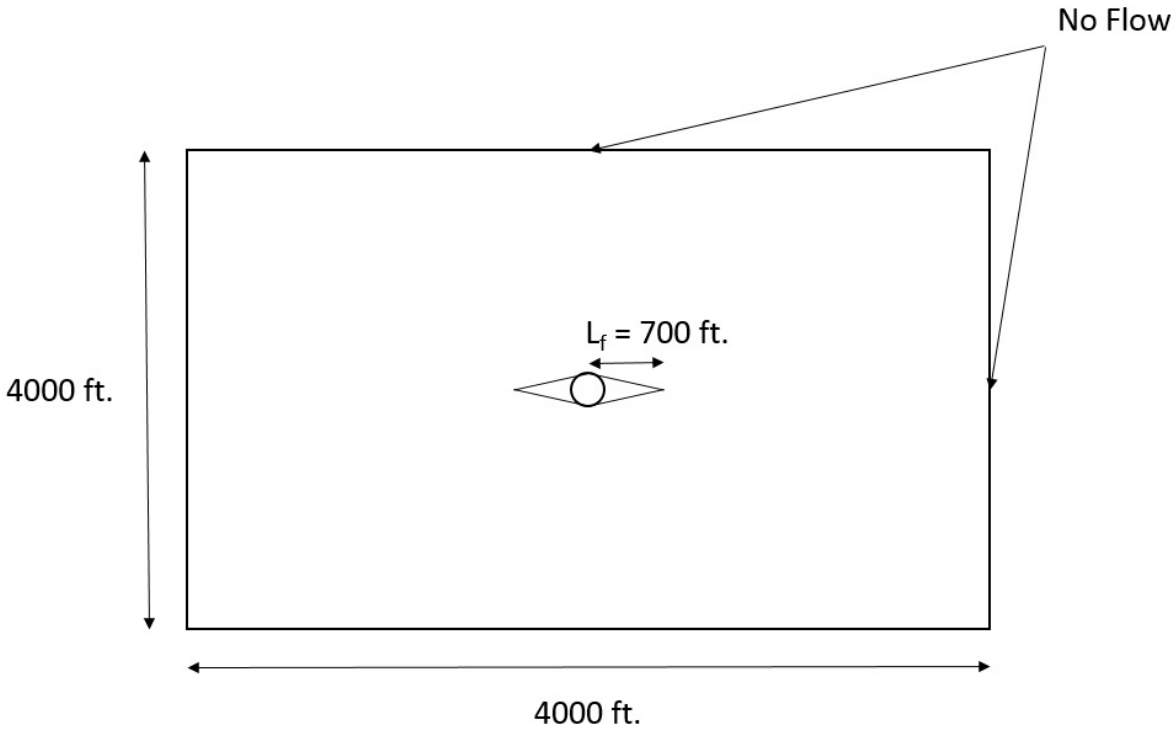

Figure 4.17: Reservoir Geometry for Synthetic Example 4

Figure 4.18 and 4.19 presents the pressure and flow rate data for this example and its duration is 450 hours. For this example, there are two drawdown and single buildup period, and for the deconvolution study, three cases will be presented by based on the whole period, buildup period and last drawdown period of pressure and flow rate data respectively. A random noise with zero mean and standard deviation of 10 B/D (σ_q) is added to the flow-rate data, as can be observed in Figure 4.19 where this is about 1 % error efficiency in the rate data. Also, a random noise with zero mean and standard

deviation of 0.01 psi (σ_p) is added to the pressure data and can be observed in figure 4.18 where this value noise is attainable today.

TABLE 4.5 – INPUT PARAMETERS FOR SYNTHETIC EXAMPLE 4	
∅, fraction	0.20
$\boldsymbol{h}$, ft	100
$\boldsymbol{c_t}$, psi^{-1}	1.0×10^{-5}
$\boldsymbol{\mu}$, cp	1
$\boldsymbol{r_w}$, ft	0.354
$\boldsymbol{C_w}$, bbl/psi	0.54
$\boldsymbol{S}$, dimensionless	1.0
$\boldsymbol{L_f}$, ft	700
$\boldsymbol{p_i}$, psi	5000
$\boldsymbol{k}$, md	100
$\boldsymbol{B_o}$, RB/STB	1

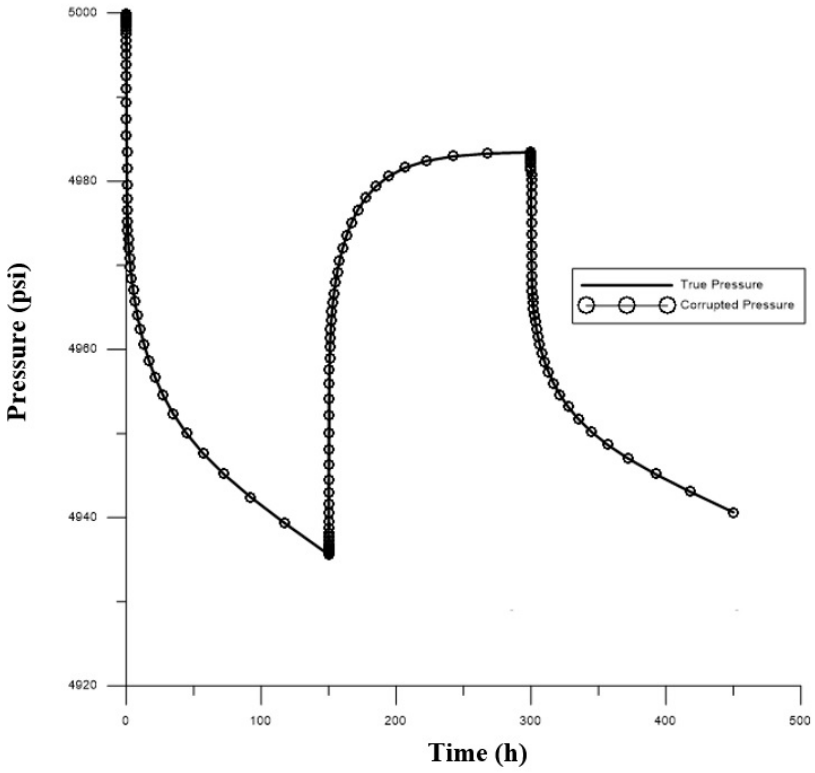

Figure 4.18: Pressure data for Synthetic Example 4

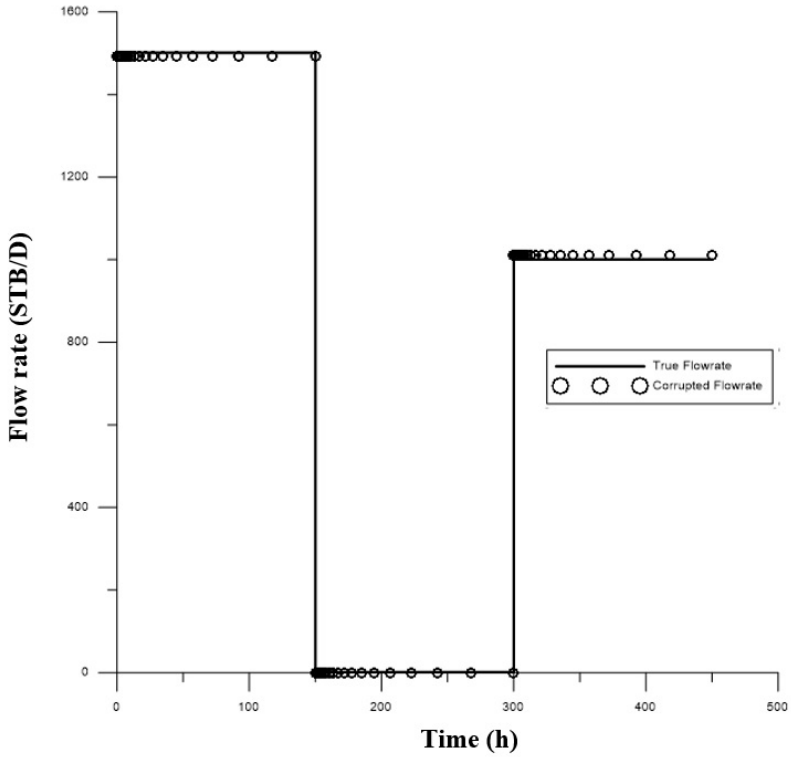

Figure 4.19: Flow rate data for Synthetic Example 4

In Figure 4.20 the true deconvolved unit response is shown for the $\sigma_p = 0.01$ psi and $\sigma_q = 10$ B/D with initial pressure is set to be 5000 psi. The curvature constraint was set to the default value which is $\sigma_c = 0.05$ in this deconvolution application. Based on figure 4.20, the wellbore storage effect is clearly identified in the early time region between 0.001 to 0.1 hours perhaps this is due to the large wellbore storage value where may indicate the wellbore is intersects with one or more induced fractures that extend some depth into the reservoir. At about 1 hour, the effect of fault is observable until the approximately ¼ slope is identified at the beginning of 5 hours until 100 hours. The ¼ slope indicate the well may encountered the bilinear flow where perhaps due to the different geological features. At the late time region, about 100 hours, the effect of the closed system boundaries is observable and could be identified by 1 unit slope.

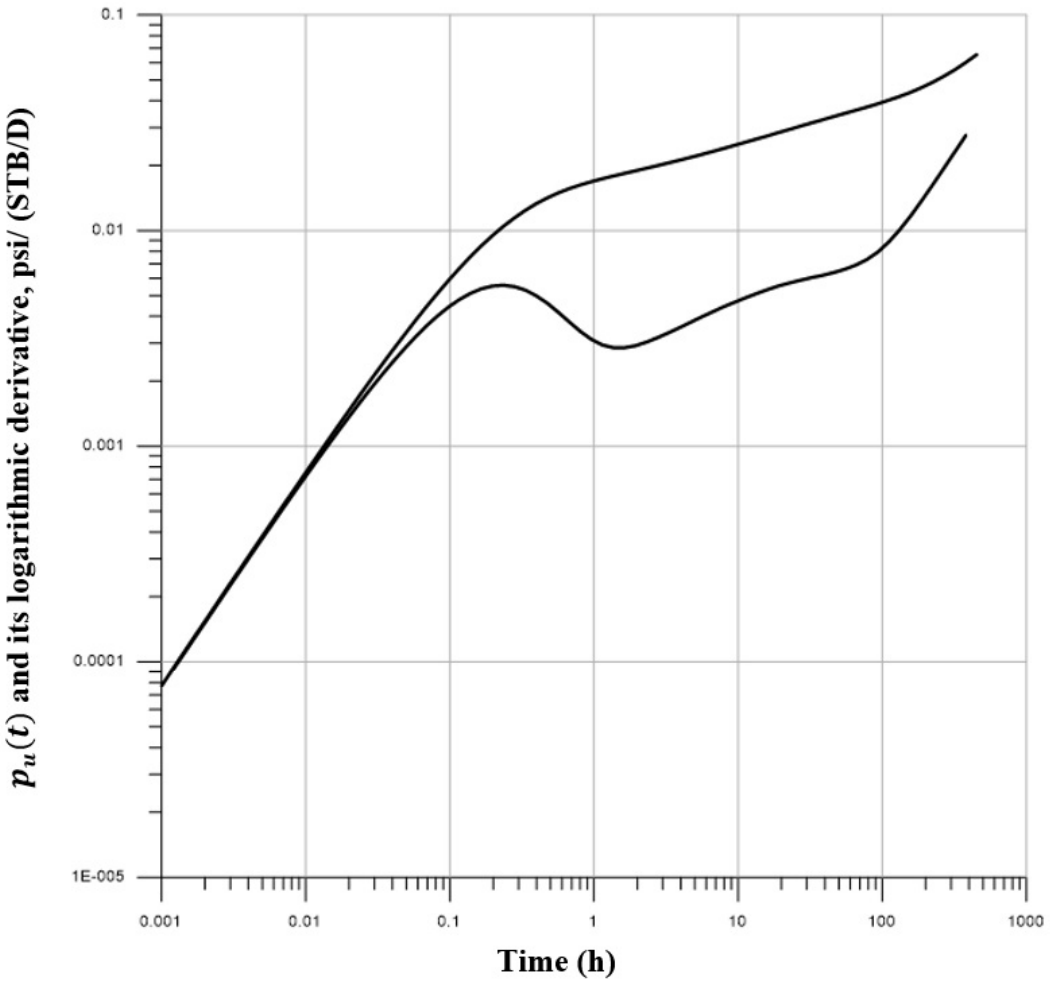

Figure 4.20: True deconvolved unit response and its derivative for Synthetic Example 4.

4.1.4.1 Case 1

In this case, pressure-rate data for the whole period sequence is used for the deconvolution study to investigate the effect of initial pressure towards deconvolved unit response. The true initial pressure of 5000 psi is added with certain percentage of noise (0.02 %, 0.1 % and 0.5 % of error) to corrupt the data and three corrupted initial pressure values are generated which are 5001 psi, 5005 psi and 5025 psi respectively. Besides, two conditions for initial pressure is implied in this study; (1) the study is conducted by assumed the value

of initial pressure is known by using the true and corrupted initial pressure values; (2) the value of initial pressure is regressed or assumed to be unknown.

In Figure 4.21, study is conducted by using the true and corrupted initial pressure values. From observation, could be identified that the deconvolved response generated based on the corrupted initial pressures have experienced signal fluctuations in the early and late time region and less successful match the true unit response but the deconvolved response generated based on true initial pressure successfully matched the true unit response. The fluctuations in the early time region may due to the effect of the noise added into the initial pressure data perhaps made it considered as inaccurate and by presence of noise in the initial pressure also, influenced the deconvolved response in late time region, thus interpretation of reservoir system hardly to be done.

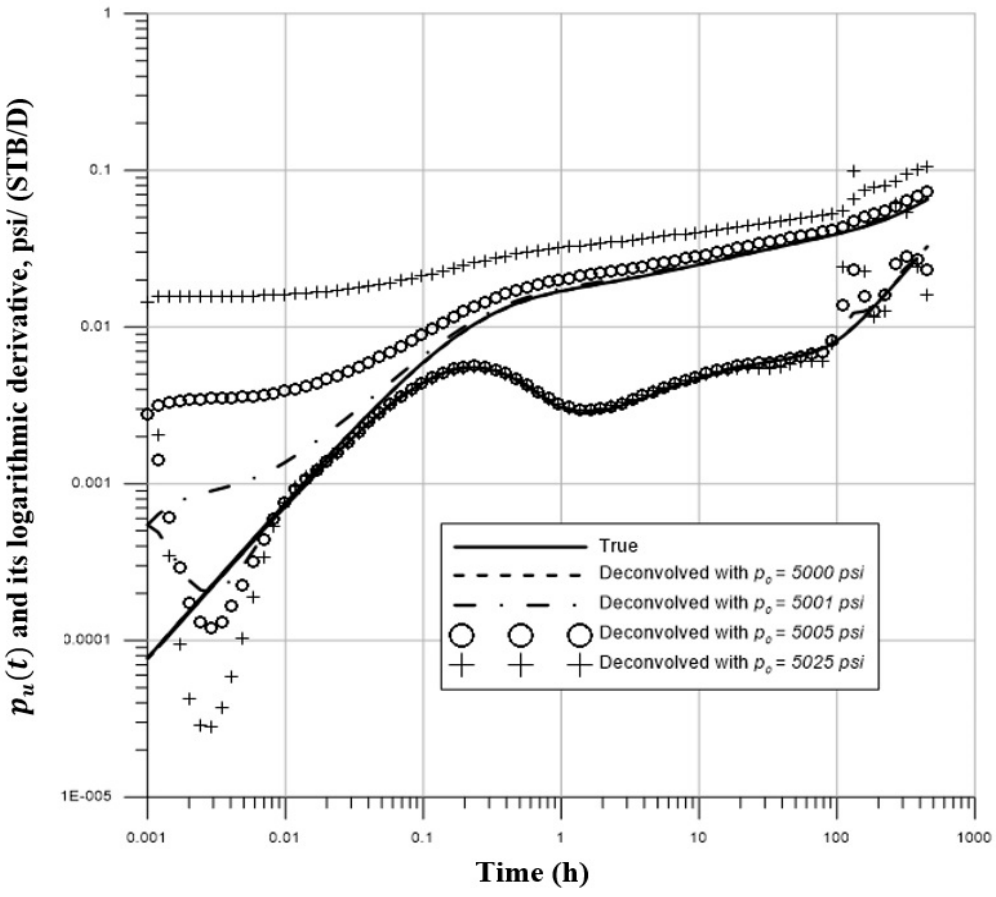

Figure 4.21: Comparison of deconvolution responses for different known initial reservoir pressures (Case 1).

The small percentage of error in initial pressure will significantly affects the deconvolved response as shown by initial pressure of 5001 psi even only contains 0.02 % of error, the deconvolved response generated from this initial pressure could not at least match the early time region of the true unit response and produce fluctuations in the early and late time region which made the analysis and interpretation of reservoir system could not be done. The maximum error percentage in initial pressure which tolerable for deconvolution algorithm to generate a good and accurate deconvolved response from the whole period sequence could be ranged less than 0.02 % of error.

Next, in Figure 4.22 is shown the deconvolved response generated from the regressed true and corrupted initial pressure or the initial pressure values are assumed as unknown. Thus, deconvolution algorithm needs to do an estimation on the initial pressure value based on the pressure-rate production history data. The value of estimated initial pressure for each run is tabulated in Table 4.6.

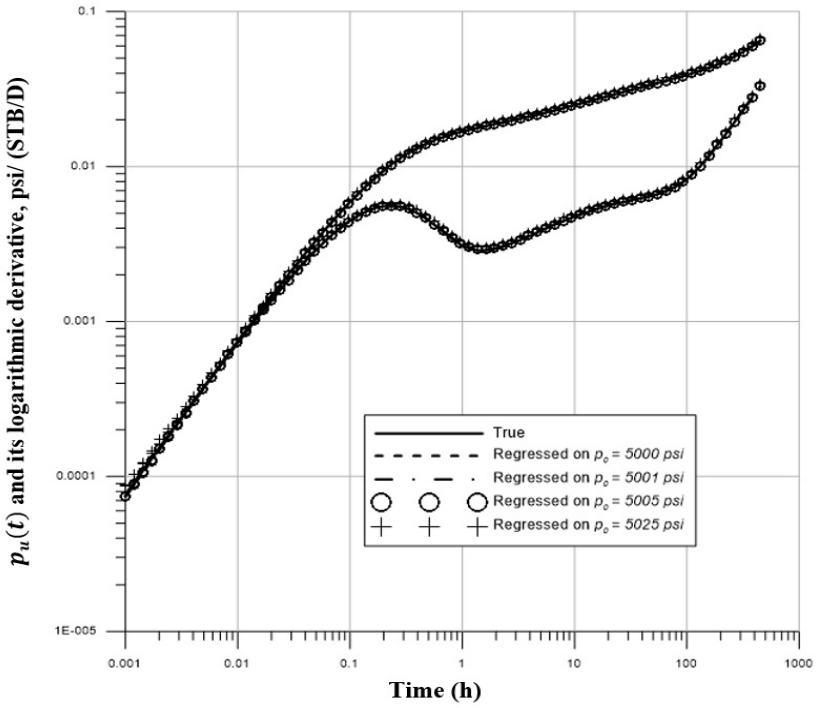

Figure 4.22: Comparison of deconvolution responses for different unknown initial reservoir pressures (Case 1).

Table 4.6: Estimated initial pressure values generated by deconvolution algorithm for Case 1.

Initial Pressure, psi	Estimated Initial Pressure, psi
5000.00	**4999.30**
5001.00	**4999.30**
5005.00	**4999.30**
5025.00	**5000.13**

Based on Figure 4.22 all the deconvolved responses are successfully matched the true unit response and no fluctuations experienced in the early and late time region compared to the test run done for the known initial pressure values. Besides, the deconvolution algorithm is done a good estimation on the initial pressure where all the estimated initial pressures are approximately close to the true initial pressure value (5000 psi). The deconvolved response generated in this run possibly could be used to analyze and interpret the reservoir system.

4.1.4.2 Case 2

In this case, the same procedure is used as Case 1 to conduct the study on the effect of initial pressure on the deconvolved response but in Case 2, only the buildup period is taking into consideration. Buildup period could be observed in Figure 4.18 and 4.19 starting from 150 hours until 300 hours. The comparison of deconvolved response between true and different initial pressure unit responses is illustrated in Figure 4.23.

In Figure 4.23, all the deconvolved responses are smoothly matched the true unit response until 1hr and at the beginning of late time region, the deconvolved responses start to deviate and shifted upwards from the true unit response perhaps this is due to the noise in

the initial pressure which lead to the inaccurate identification of reservoir boundary in late time region.

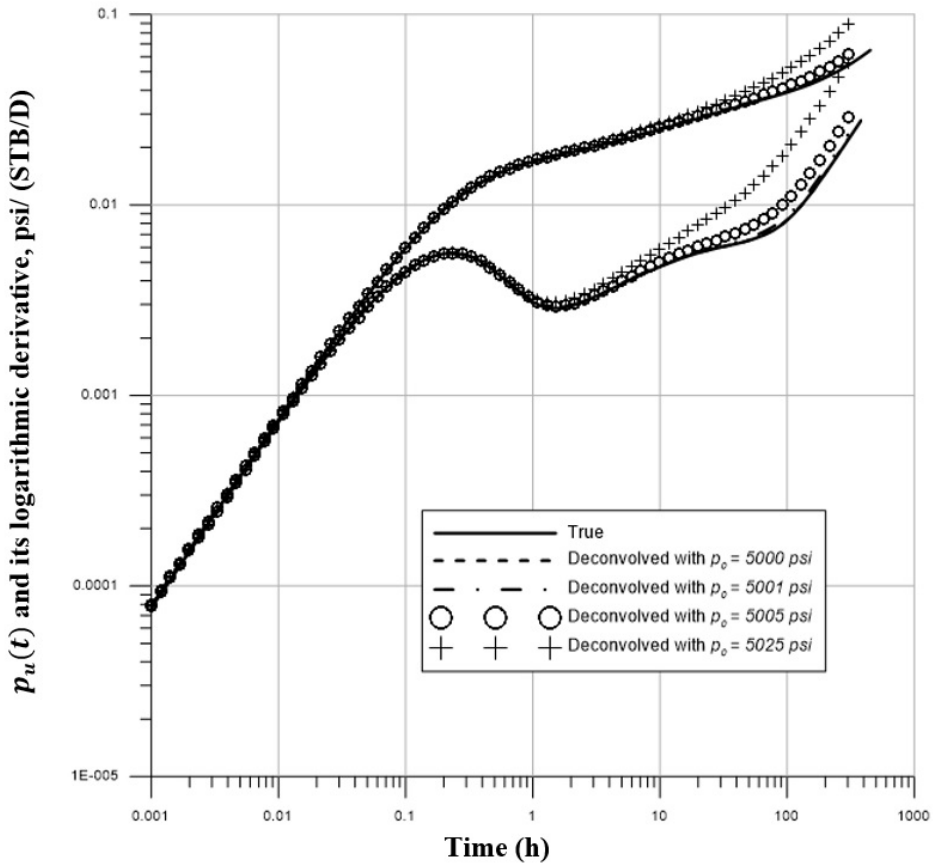

Figure 4.23: Comparison of deconvolution responses for different known initial reservoir pressures (Case 2).

Also, by only considered buildup period to generate the deconvolved response, deconvolution algorithm could highly tolerate with error percentage presence in the initial pressure compared to the Case 1 which consider the whole period sequence of pressure-rate data. Deconvolved response generated from initial pressure of 5000 psi and 5001 psi is approximately matched the true unit response by using buildup period data, thus, this could be taken into account that the maximum error percentage which tolerable for deconvolution algorithm if only buildup period is taking into consideration, is 0.02 % of error.

For the study done by using regressed initial pressure data is illustrated in Figure 4.24 and the estimated initial pressure values is tabulated in Table 4.7.

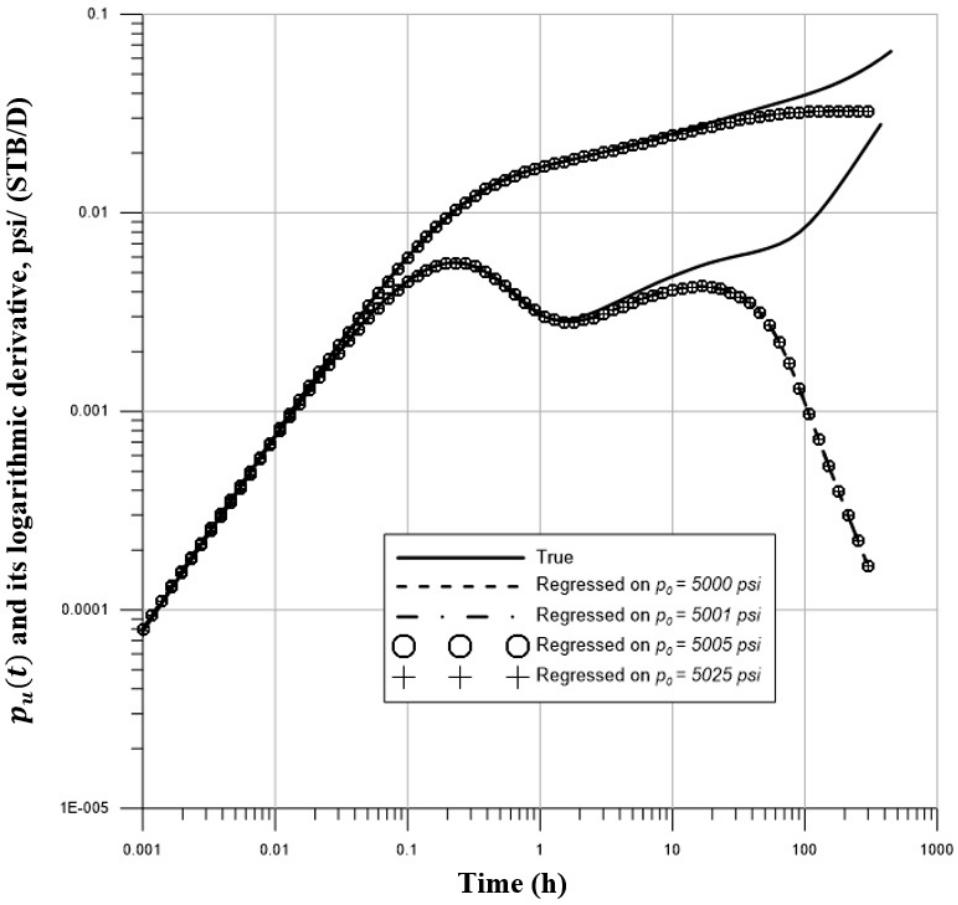

Figure 4.24: Comparison of deconvolution responses for different unknown initial reservoir pressures (Case 2).

Table 4.7: Estimated initial pressure values generated by deconvolution algorithm for Case 2.

Initial Pressure, psi	Estimated Initial Pressure, psi
5000.00	**4983.84**
5001.00	**4983.84**
5005.00	**4983.84**
5025.00	**4983.84**

The estimated initial pressure generated by deconvolution algorithm by only using buildup period pressure-rate data is approximately close to the 5000 psi which is the true initial pressure but unfortunately the deconvolved pressure response for all initial pressure values could not matched the true unit response in late time region even it is perfectly matched in early and middle time region. In late time region could be seen that the deconvolved response is deviated and shifted downwards where this behavior of signal is telling that the reservoir is having a buildup process and also this proved that, by only using buildup period data, it is insufficient to identify the whole reservoir system because build up period data less capable to estimate the reservoir boundary behavior compared to the whole period sequence data.

4.1.4.3 Case 3

In this case, the same procedure is used as Case 1 and Case 2 where to conduct the study on the effect of initial pressure on the deconvolved response but in this case, the last drawdown period is taking into consideration. The last drawdown period could be observed in Figure 4.18 and 4.19 which is run for 150 hours duration starting from 300 hours until 450 hours. The comparison of deconvolved response between true and different initial pressure unit responses is illustrated in Figure 4.25.

Based on Figure 4.25, the same behavior of deconvolved responses could be observed as in Case 2 where all the initial pressure deconvolved response is smoothly matched the early and middle time region but deviation of signal is experienced in late time region perhaps this is also due to the noise presence in the initial pressure data and this will lead to misinterpretation of reservoir system. In the true unit response, it is shown that the reservoir will experience a reservoir boundary effect in late time region by given out a signal of 1 unit slope but unfortunately in Figure 4.25, the signal shown ¼ slope which could be analyzed as bilinear flow and the reservoir did not experience the boundary effect. From the study conducted, if only last drawdown period of pressure-rate data is used, the best deconvolved responses could be generated by having a maximum percentage of error in initial pressure of less than 0.02 %.

In Figure 4.26, it is shown the comparison of deconvolution responses for different unknown initial pressure or regressed initial pressure. Besides, Table 4.8 is the tabulated data for estimated initial pressure value done by the deconvolution algorithm. As in the previous cases, the estimated initial pressure generated by deconvolution algorithm is approximately close towards the real initial pressure and the estimation is done based on the pressure-rate production history data.

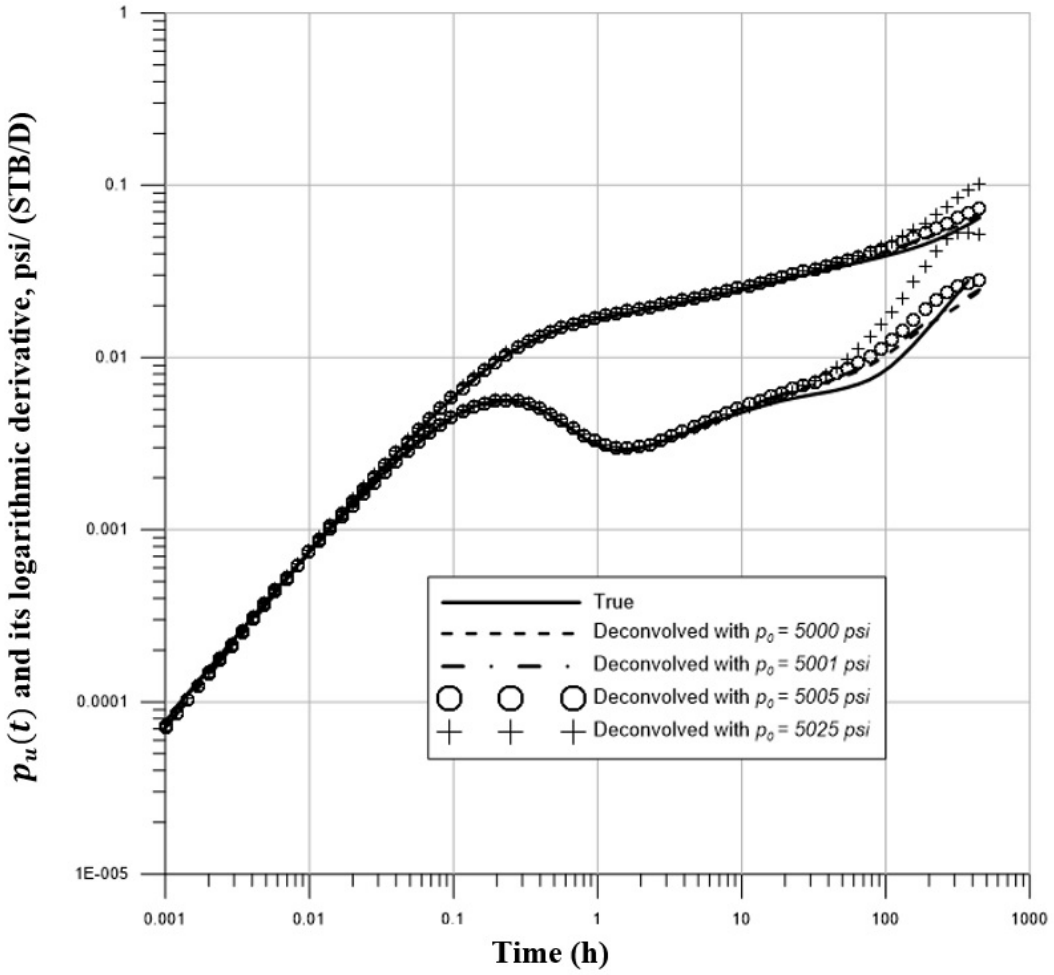

Figure 4.25: Comparison of deconvolution responses for different known initial reservoir pressures (Case 3).

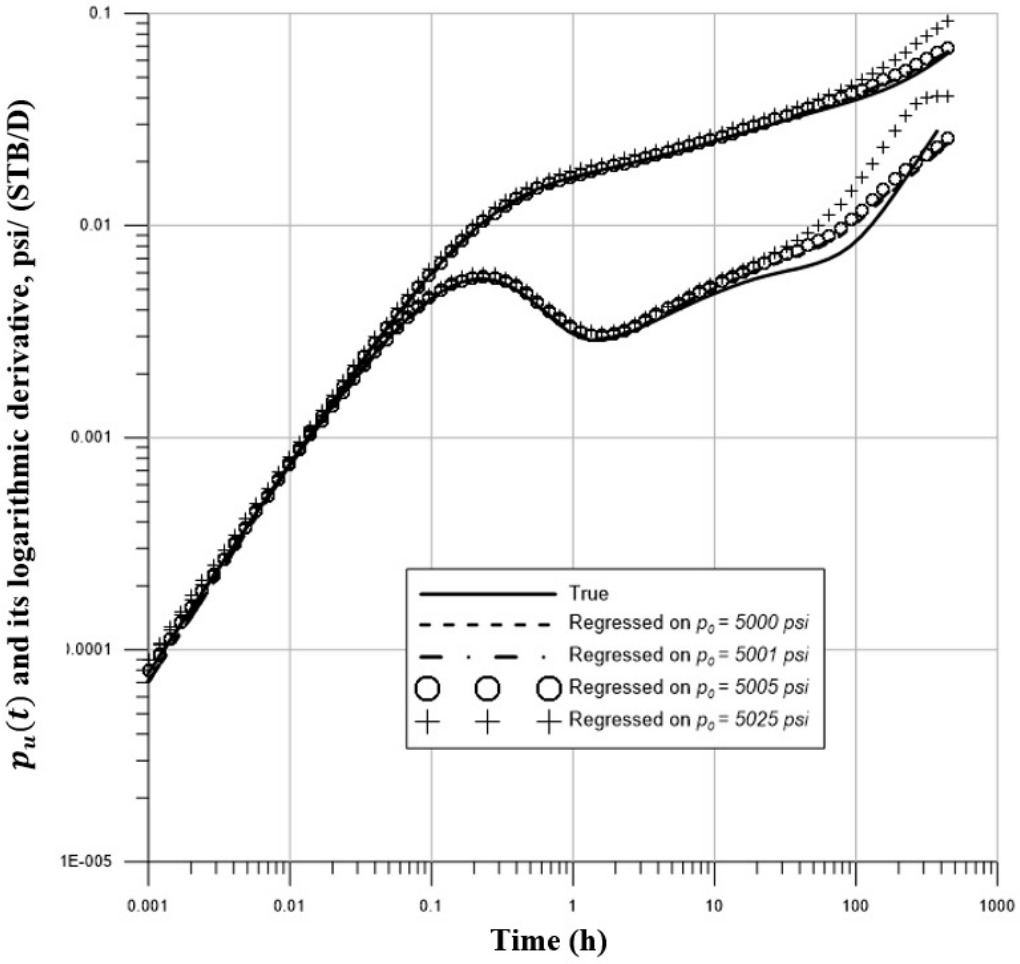

Figure 4.26: Comparison of deconvolution responses for different unknown initial reservoir pressures (Case 3).

Table 4.8: Estimated initial pressure values generated by deconvolution algorithm for Case 3.

Initial Pressure, psi	Estimated Initial Pressure, psi
5000.00	**4999.79**
5001.00	**5000.28**
5005.00	**5001.67**
5025.00	**5016.34**

In Figure 4.26, the result of deconvolved responses is almost identical with the deconvolved responses generated by using known initial pressure as shown in Figure 4.25. The signals are shifted upwards by given ¼ slope in late time region and totally deviated from the true unit response which represents late time region by 1 unit slope. This signal deviation will lead to the misinterpretation of reservoir system and reservoir boundary.

Based on the three cases, could be conclude that the value of initial pressure do significantly affect the deconvolved response and there is certain level of maximum error in the initial pressure which could be tolerable for deconvolution algorithm. In the real application, incorrect or inaccurate initial pressure data will generate an incorrect deconvolved response and analysis of reservoir system also may lead to be inaccurate. Although, fortunately the recent robust deconvolution algorithm has an ability to forecast or estimate the initial pressure data based on the pressure-rate production history and this ability also in the same time could correct the inaccurate initial pressure.

Chapter 5

Conclusions and Recommendations

The objective of this research is to study the effects of the algorithmic parameters (including error levels in pressure and rate data, and the curvature constraint value) as well as the initial pressure on the deconvolved responses by using the recent robust deconvolution algorithm of Pimonov et al. and/or the ones implemented in Weatherford PanSystem Test Software and to test the proposed deconvolution algorithm for the effectiveness and efficiency.

Based on the basis of this work, from the sensitivity study of the number of nodes could conclude that the number of nodes can affect the deconvolved pressure response results in terms of the quality and coarseness. Besides, the regularization parameter as investigated in Synthetic Example 2 do effect on the derivative smoothness term when the TLS method is used in the deconvolution algorithm. The optimization of flow rates which modified the flow rates during the deconvolution process does not significantly affecting the deconvolved derivative results because it just adding the weighting value for the optimization of the rate term in the TLS method.

In Synthetic Example 3, the investigation of relationship between error efficiency percentages with deconvolved response for each of recent robust deconvolution algorithms (von Schroeter et al. and Pimonov et al.) shown that percentage of error efficiency do effect the deconvolved response and each algorithms have its own percentage of error tolerant. Based on this Example 3, Pimonov et al. shown their algorithm is more tolerant towards noisy data compared to von Schroeter et al. algorithm, and provide a promising deconvolved response to identify the reservoir model and its flow regimes.

Besides, from sensitivity study done in Synthetic Example 4, the initial pressure is do significantly affect the deconvolution response and deconvolved derivative response. A presence of small percentage of error in the initial pressure data or by provide inaccurate initial pressure data as an input will generate a unreliable deconvolved response where open the chances for misinterpretation and wrong analysis of reservoir system. As an alternative for the inaccurate or unknown initial reservoir pressure data, the recent robust deconvolution algorithm is equipped with a 'remedy' where it could correct and estimate the initial reservoir pressure data based on the pressure-rate production history data.

From both synthetic examples, Pimonov et al. algorithm shows the reliability and robustness in generating the high quality deconvolved derivative results which almost identical to the true pressure response model compared to the algorithm implemented in the Weatherford PanSystem. In the future, this sensitivity study of the algorithmic parameters (including error levels in pressure and rate data, and the curvature constraint value) as well as the initial pressure on the deconvolved responses by using the recent robust deconvolution algorithm could be used as a base to ensure the robustness of the algorithm and to improve the effectiveness and efficiency of deconvolution algorithm.

References

[1] Baygun, B., Kuchuk, F.J., and Arikan, O.: “Deconvolution under Normalized Autocorrelation Constraints,” SPEJ (September 1997) 246.

[2] Bostic, J., Agarwal, R. and Carter, R.: “Combined Analysis of Postfracturing Performance and Pressure Buildup Data for Evaluating an MHF Gas Well,” JPT 32(10), 1711-1719, (1980).

[3] Bourdet, D., Ayoub, J.A., and Pirard, Y.M.: “Use of Pressure Derivative in Wel Test Interpretation,” SPE Form Eval 4(2): 293-302; Trans., AIME (1989), 287.

[4] Coats, K.H., Rapoport, L.A., McCord, J.R., and Drews, W.P.: “Determination of Aquifer Influence Functions From Field Data,” JPT (December 1964) 1417; Trans, AIME, 231

[5] Gajdica, R., Wattenbarger, R., and Stratzman, R.: “A New Method of Matching Aquifer Performance and Determining Original Gas in Place,” SPE Formation Evaluation, 3(3), 985-994, (1988).

[6] Gringarten, A.C.: “From Straight Lines to Deconvolution: The Evolution of the State of the Art in Well Test Analysis,” paper SPE 102079, SPE Annual Technical Conference and Exhibition, (2008).

[7] Hutchinson, T., and Sikora, V.: “A Generalized Water-DriveAnalysis,” Trans, AIME (1959), 216, 169-177

[8] Ilk, D., Valko, P.P., and Blasingame, T.A.: “Deconvolution of Variable-Rate Reservoir Performance Data Using B-Splines,” paper SPE 95571 presented at the 2005 SPE Annual Technical Conference and Exhibition, Dallas, TX, 9-12 October.

[9] Jargon, J.R. and van Poollen, H.K.: “Unit Response Function From Varying Rate Data,” JPT (August 1965) 965; Trans. AIME, 234

[10] Kuchuk, F., and Ayestaran, L.: “Analysis of Simultaneous Measured Pressure and Sandface Flow Rate in Transient Testing,” JPT 37(2), 23-334, (1985).

[11] Kuchuk, F.J., Onur, M., Hollaender, F.: “Pressure Transient Formation and Well Testing: Convolution, Deconvolution and Nonlinear Estimation,” Elsevier, (2010).

[12] Kuchuk, F.J.: “Application of Convolution and Deconvolution to Transient Well Tests,” SPEFE (December 1990) 375.

[13] Levitan, M.M.: “Practical Application of Pressure/Rate Deconvolution to Analysis of Real Well Tests,” SPEREE (April 2005) 113.

[14] Onur, M., Cinar, M., Ilk, D., Valko, P.P., Blasingame, T.A. and Hageman, P.S.:”An Investigation of Recent Deconvolution Methods for Well-Test Data Analysis,” SPEJ 13(2): 226-247. SPE-102575-PA. DOI: 10.2118/102575-PA (2008).

[15] Pascal, H.: “Advances in Evaluating Gas Deliverability using Variable Rate-Tests under Non-Darcy Flow,” paper SPE 9841, SPE/DOE Low Permeability Symposium, (1981).

[16] Pimonov, E., Ayan, C., Onur, M., and Kuchuk, F.J.: “A New Pressure/Rate Deconvolution Algorithm to Analyze Wireline Formation Tester and Well Test Data,” SPE Res. Eval. & Eng., vol. 13(4), pp. 603-613,(2010).

[17] Pimonov, E., Ayan, C., Onur, M., and Kuchuk, F.J.: “A New Pressure/Rate Deconvolution Algorithm to Analyze Wireline Formation Tester and Well Test Data,” paper SPE 123982 presente at SPE Annual Technical Conference and Exhibition, New Orleans, 4-7 October, (2009b).

[18] Pimonov, E.A., Onur, M., and Kuchuk, F.J.: “A New Robust Algorithm for Solution of Pressure/Rate Deconvolution Problem,” J. of inverse and Ill-posed Problems 17(6): 611-627, (2009a).

[19] Roumboutsos, A. and Stewart, G.: “A Direct Deconvolution or Convolution Algorithm for Well Test Analysis,” paper SPE 18157, SPE Annual Technical Conference and Exhibition, (1988).

[20] Thompson, L.G. and Reynolds, A.C.: “Analysis of Variable-Rate Well-Test Pressure Data Using Duhamel’s Principle,” SPEFE (October 1986) 453.

[21] Van Everdingen, A.F. and Hurst, W.: “Application of the Laplace Transform to Flow Problems in Reservoirs,” Trans., AIME (1949), 186.

[22] von Schroeter, T., Hollaender, F., and Gringarten, A.C.: “Analysis of Well Test Data From Downhole Permanent Downhole Gauges by Deconvolution,” SPE 77688 presented at the 2002 SPE Annual Technical Conference and Exhibition, San Antonio, Texas, 29 September-2 October.

[23] von Schroeter, T., Hollaender, F., and Gringarten, A.C.: “Deconvolution of Well Test Data as a Nonlinear Total Least Square Problem,” SPEJ (December 2004) 375.